EUROPEAN COMMISSION
Community Research

SEVENTH FRAMEWORK PROGRAMME

CARBOWASTE

Treatment and Disposal of Irradiated Graphite and Other Carbonaceous Waste

Grant Agreement Number: FP7-211333

Deliverable (D-4.3.6)
Decontamination factors by treatment with oxygen

Author(s): Lorraine McDermott, Greg Black, Robert Worth and William Bodel;
University of Manchester
Kathrin Baginski and Dirk Vulpius;
Forschungszentrum Juelich GmbH

Supervisor(s): Abbie Jones and Barry Marsden; University of Manchester

Reporting period: e.g. 01/04/2008– 31/03/2013

Project co-funded by the European Commission under the Seventh Framework Programme (2007 to 2012) of the European Atomic Energy Community (EURATOM) for nuclear research and training activities

Date of issue of this Report: 28/02/2013

Start date of project : **01/04/2008** Duration : **53 Months**

Dissemination Level		
PU	Public	
RE	Restricted to the partners of the CARBOWASTE project	**X**
CO	Confidential, only for specific distribution list defined on this document	

Distribution list

Person and organisation name and/or group	Comments
Task 4.3 members	
Executive Board	
Co-ordinator	

CARBOWASTE		
Work package: 4 **Task: :** 4.3	**CARBOWASTE document no:** CARBOWASTE-1302-D-wp4.Deliverable D-4.3.6. (e.g. May 2008 as date of issue: 0805)	**Document type:** Deliverable
Issued by: Lorraine McDermott **Internal no.:** UoM_WP4_D4.3.6_Final		**Document status:** Final

Document title
Decontamination factors by treatment with oxygen

Executive summary

This deliverable focuses on the research carried out within the CARBOWASTE program on thermal treatment of i-graphite under inert and oxygen environments.

This report will provide background information on the i-graphite providence, reactor operational parameters and isotopic inventory present within irradiated graphite in order to understand and determine the effects of thermal treatment. The thermal treatment experiments have focused on oxygen environments compared to inert in order to establish baseline isotopic release rates & the effects on increased time within thermal treatment environments. This research contribute to further understanding isotopic release, location and evaluations whether pursing this research in the future may result in mechanistic understand of isotopic release from i-graphite or provide a possible decommissioning option for certain i-graphite sources.

Revisions

Rev.	Date	Short description	Author	Internal Review	Task Leader	WP Leader
00	15/02/2013	First Issue	McDermott, UoM	Baginski, FZJ		
01	22/02/2013	2nd issue	McDermott, UoM	Baginski, FZJ		
02	28/02/2013	Final Issue	McDermott, UoM Baginski, FZJ	Marsden, UoM Jones, UoM	Vulpius, FZJ	Vulpius, FZJ

Table of Contents

TABLE OF CONTENTS 4

1 INTRODUCTION 7

1.1 Aims and Objectives of Deliverable 7

1.2 Thermal Treatment 7

1.3 Literature Data Available 8

1.4 Key Radionuclides of Concern 10

1.5 Sources of i-graphite 10

2 FZJ 11

2.1 Methodology & Instrument set up 11

2.2 Gas Detection Techniques 13

2.3 I-graphite material from the Merlin material test reactor 15

2.4 Isotopic inventory in Merlin i-graphite 16

2.5 Saint Laurent A 2 Graphite 18

2.6 Experimental results FZJ 24

2.7 Thermal treatment parameters 32

2.8 Conclusions from FZJ work 32

3 UOM 34

3.1 Experimental Program 34

3.2 Oldbury Graphite 36

3.3 Treatment Program 38

3.4 Thermal treatment isotopic release 39

3.5 Post Treatment Analysis 43

3.6 XRD 44

3.7 Gamma Spectroscopy 48

3.8 Autoradiography 54

3.9 Helium pycnometry 58
3.10 Surface Area 62
3.11 Conclusions from UoM work 65
4 SUMMARY 67
4.1 Publications resulting from this work 68
5 REFERENCES 69

Table of Abbreviations

Symbol / Abbreviation / Acronym	Definition
α	Alpha
AGR	Advanced Gas-cooled reactor
BEPO	British Experimental Pile Zero Reactor
β	Beta
CEA	Commissariat à l'énergie atomique et aux énergies alternatives
CoRWM	Committee On Radioactive Waste Management
ε	Electron capture
EDF	Electricité de France
EDND	Equivalent DIDO Nickel Dose
ENEA	Italian National Agency for New Technologies
FNAG	Furnaces Nuclear Application Grenoble
FZJ	Forschungszentrum Jülich
γ	Gamma
GDF	Geological Disposal Facility
GLEEP	Graphite Low Energy Experimental Pile
HOPG	Highly ordered pyrolytic graphite
HAW	High Activity Waste
IAEA	International Atomic Energy Agency
ICRP	International Commission on Radiological Protection
ILW	Intermediate Level Waste
INPL	Institute of Nuclear physics of Lyon
i-graphite	Irradiated graphite
LLW	Low Level Waste
LLWR	Low Level Waste Repository
LSC	Liquid Scintillation Counting
MW	Megawatt
MW(th)	Megawatt Thermal
n	neutron
NCRP	National Council on Radiation Protection and Measurements
NDA	Nuclear Decommissioning Authority
NNL	National Nuclear Laboratory
NRG	Nuclear Research and consultancy Group
p	proton
PGA	Pile Grade A
pH	measure of the acidity or basicity of an aqueous solution
PIE	Post Irradiation Examination
σs	scattering cross-section
σa	absorption cross-section
SoGIN	SOcietà Gestione Impianti Nucleari
TRL	Technology Readiness Level
UKAEA	United Kingdom Atomic Energy Authority
UoM	University of Manchester
VLLW	Very Low Level Waste

1 Introduction

1.1 Aims and Objectives of Deliverable

To date there is little published work reported in the open literature which investigates the impact of thermal treatment, characterisation parameters and resulting isotopic release on irradiated graphite from commercial large scale graphite moderated reactors, this CARBOWASTE deliverable aims to bring together previous work published as well as new research carried out at both UoM & FZJ laboratories.

1.2 Thermal Treatment

The first example of thermal treatment and disposal of nuclear graphite is the Graphite Low Energy Experimental Pile (GLEEP) [1]. No radiological characterisation parameters are documented in this report, however GLEEP graphite is reported as LLW. The successful disposal of graphite from the GLEEP reactor using this methodology indicates graphite decommissioning using thermal treatment is a viable option [2-3]. GLEEP graphite blocks were thermal treated in an industrial incinerator at 1423K for approximately 3 hours under a forced air supply. It is noted there is also the presence of other miscellaneous waste within the incinerator. Typically, 87% of tritium and 63% ^{14}C activity were removed from each block and a very crude net weight loss assessment of 6% calculated post-treatment.

1.3 Literature Data Available

Studies conducted by FJZ (Germany) [4] have examined the corrosion behaviour of graphite under final repository conditions. Characterisation parameters included structural assessment of density, thermal conductivity, Young's Modulus, Thermal Expansion co-efficient and electrical resistivity. Radiochemical experiments were performed to assess the isotopic inventory using Gas-Chromatography mass spectroscopy, Optical and electron microscopy, surface area (BET), Gamma spectroscopy and X-ray diffraction. Thermal treatment showed that the highest concentration of ^{14}C is bonded to the surface and therefore is loosely bound in chemical terms. Chemical treatment have proved this ^{14}C may be removed from the ^{12}C through thermal treatment with Ar / O_2 [5]. These initial studies concluded that up to 60% of the ^{14}C and 80% of the tritium may be removed with a mass loss to the ^{12}C of only 5%. Although these studies are in their infancy, there is scope within FZJ to scale this up to a pilot treatment plant and the group are confident to achieve up to 95% ^{14}C loss in future experiments [6].

The recent international collaborative program: CARBOWASTE examines pyrolysis and thermal treatment further within the Treatment and Purification work package. Reactive gases such as Chlorine and Oxygen have been identified and are undergoing considerable investigation. The thermal radionuclide release could be increased by steam or other reactive gases (oxygen, halogens, hydrogen). However, this could lead to an increase of the graphite oxidation therefore; the influence of these components will be studied with respect to the radionuclide release rates and optimised with respect to a minimised graphite oxidation.

Steam Reformation has been proposed by Studsvik, and Bradbury [1] where the company quotes:
"graphite fragments are transformed by high temperature interaction with steam into two combustible gases (hydrogen and carbon monoxide). The gas treatment at the outlet of the reformer consists of a quencher, a scrubber, and a water condenser. After

oxidation and transformation into CO_2 and H_2O, the gas is released to the atmosphere through a HEPA filter." [7]

This published work claims "approximately 1200 tonnes of graphite" could be transformed into 10000 tonnes of calcium carbonate or 20000 tonnes of barium carbonate, which is very insoluble and prevents the release of radionuclide's into the environment [8] however initial volume reduction and radiological assessment is required.

Studsvik Inc. have a demonstration Steam Pyrolysis plant at Erwin, Tennessee with which Bradtec is a collaborator [9]. Studsvik have performed extensive work on processing low level radioactive waste via a patented Thermal Organic Reduction (THOR) process. THOR is a combined pyrolysis / steam reforming, fluidised bed treatment system [1]. THOR can process liquid, solid or slurry low level active waste. Studsvik claim THOR can offer consistent, reliable, robust operating characteristics with a volume reduction up to 80:1 and weight reductions up to 100:1 when processing is complete. Typical radionuclide partitions are used to separate ^{14}C, ^{3} A safety aspect advantage of THOR includes the plant housed in tightly controlled containment and therefore any loss of hazardous gases or materials are reduced significantly. Other advantages of this system include removal of Wigner energy, retention of gasified carbon for further processing if necessary, and separation of graphite (carbon) from radioactive contaminants and possible in-situ treatment of graphite from reactor core.

There is one final characteristic of decontamination by heating [8]. If the carbon in graphite is completely gasified (e.g. by steam reformation or air oxidation) the remaining non-volatile isotopes will be left behind as a residue, while semi-volatile isotopes (such as ^{137}Cs) may be collected with the non-volatile ones, or in adjacent low temperature zones. This behaviour has been confirmed in the Jülich study [4]. Total gasification provides the means to collect these isotopes in a concentrated form for waste management. This is a significant outcome, since the non- and semi-volatile isotopes include all the principal gamma-emitting ones. This allows all further downstream operations with the carbon to be performed "hands on". The separation of

volatile non-carbon isotopes such as tritium and ^{14}C can be readily accomplished during gas phase processing: for example tritium can be converted to water and separated from the off gas, carbon dioxide; this off gas could incorporate with future carbon sequestration programs.

1.4 Key Radionuclides of Concern

The focus of thermal treatment is in removing long lived beta isotopes from i-graphite. This technique has been used for isotopic determination of ^{3}H and ^{14}C within i-graphite for several years, upon complete combustion of the i-graphite sample the gamma isotopes remain the in combustion boat. This allows the separation of the waste stream as gamma and beta isoptes has significantly different half lives, energies and radiological hazards.

Separating ^{3}H, ^{14}C, ^{36}Cl from ^{60}Co, ^{63}Ni, ^{90}Sr, ^{133}Ba, ^{134}Cs, ^{137}Cs, ^{152}Eu, ^{154}Eu opens up other waste disposal opportunities as well as bring in other technologies such as carbon capture.

1.5 Sources of i-graphite

The application of thermal treatment on i-graphite considers that all i-graphites are suitable for thermal treatment but the graphite source and irradiation history will have to be considered. The graphite samples from Merlin reactor appear to be most effective for thermal release. The so called Merlin (FRJ-1) reactor was a swimming pool reactor operating at temperatures far below 100°C. For the Oldbury Reactor 2 samples provided by NNL there has already been a significant weight loss in the mass of the graphite during reactor operation. Oldbury Reactor 2 was a CO_2-cooled reactor operating at higher temperatures 543K region therefore volatile radionuclides may have been already released during operation. This would conclude that the thermal treatment may not so effective in the amount of released species for some i-graphites.

2 FZJ

2.1 Methodology & Instrument set up

Initial experiments at FZJ, photograph shown in figure 1, established that pure nitrogen flow gas and a ceramic tube with overnight furnace heating (to reduce experimental run times) weren't sufficient as sample placement in the furnace exposure the material to the atmosphere and changed what was thought to be an inert experiment to an experiment with oxygen input at the start of the test.

Following on from these initial experiments nitrogen gas with defined oxygen content in a range of 0,1% to 1% was flushed through the system with a defined gas flow adjusted at a gas flow controller. The sample was placed in a tube furnace with a sample holder at ceramic tube tests and without a sample holder in quartz tubes. Volatile radionuclides were caught in the washing bottles. The washing bottles were constructions build in collaboration of the glass manufacturing department of Research Center Juelich, see schematic in Figure 2. The essential characteristic of the washing bottles is that every washing bottle has to be fixed on stands so that defined sample solution can be taken while the test is running with two outlet valves at the bottom of the bottle. The first two washing bottles was filled with 50 ml 0.1 mol/l nitric acid. Tritium as HTO was absorbed in the first two bottles. After this two washing bottles the concentration of CO, CO_2 and O_2 in gas flow was detected by the gas analyser of Emerson Process Management. After the analysing system two washing bottles to capture CO_2- radiocarbon were connected. Then carrier with off-gases passed through a CuO-catalyst reactor tube at a temperature of 550°C in order to oxidise tritium, also presenting as tritiated molecular hydrogen in the gas mixture, and carbon monoxide CO_2 correspondingly. Oxidised molecular hydrogen was absorbed in the fifth and sixth bottles with 0.1 mol/L nitric acid. At the catalyst oxidized CO passed the bottles before it was absorbed in the seventh and eighth washing bottles as CO_2, which are filled with 50 mL 4 mol/L NaOH. At defined temperature during the experiment, samples of the solutions in the washing bottles, every sample taking time 3 mL, have been taken from washing bottles in defined time intervals. With liquid

scintillation measurement counting the content of tritium and radiocarbon was detected in the solutions. So radionuclide release at defined time of testing could be determined.

Determination of sample mass loss during real time detection CO and CO_2 concentration by IR spectrometer from the gas flow was unsuccessful as uncertainties of measuring and equipment were too large to determine values without sample weighing which wasn't possible in-situ.

Figure 1 Photo of FZJ equipment used for thermal treatment

The measurement the off- gases during incineration was achieved using special measurement cells suitable for infrared (CO, CO_2) or paramagnetic detection (O_2).

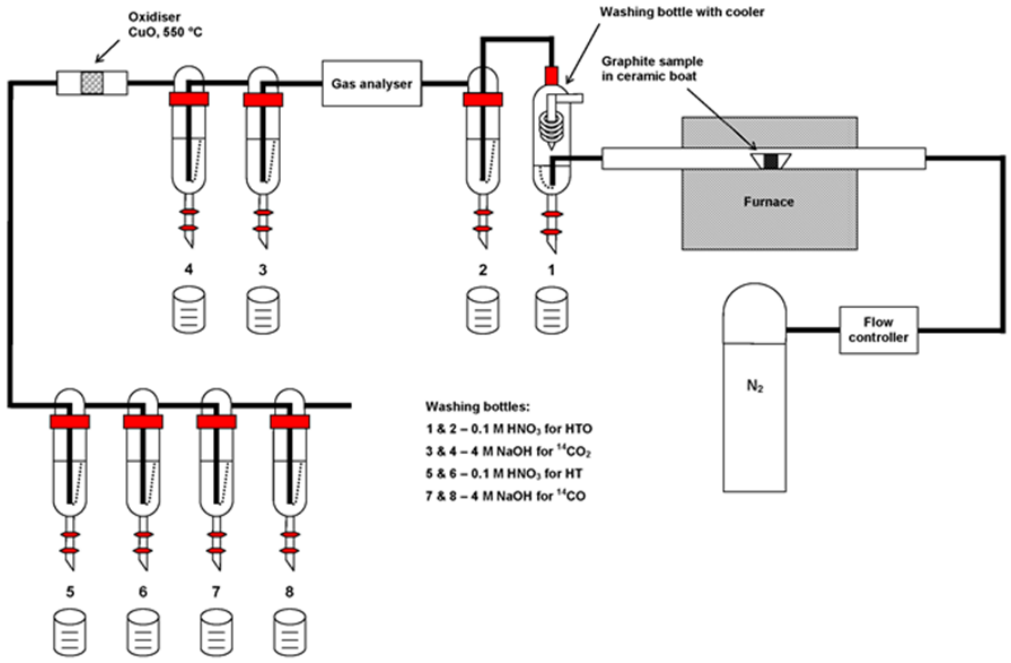

Figure 2 Schematic of FZJ equipment used for thermal treatment

2.2 Gas Detection Techniques

Gas detection during thermal treatment was realised with a multi-component-analyzing tool called MLT-Series of the NGA 2000 product family of Emerson Process Management Company. Different measurement methods are combined in one measurement device. The special measurement device designed for thermal treatment equipment contains measurement modules for oxygen, carbon monoxide, carbon dioxide, hydrogen and methane. Every twenty seconds the concentration in ppm is measured. For oxygen measuring two detection methods are available; a paramagnetic sensor measuring in the range of percent and an electrochemical sensor measuring in the range of ppm. With paramagnetic measurement detection method oxygen can be detected quick and easy. The O_2-molecule has two unpaired electrons so in a magnetic field oxygen shows magnetic attraction force. In the paramagnetic measurement cell two spheres were mounted on a turning device in a magnetic field. Centrally between these spheres a mirror is fixed. On these mirror a light source is focused. If the oxygen passes the measurement cell the spheres will be deflected. The amount of deflection is measured with photo cells by the reflecting light.

The signal the photo cells receive will be transformed into electrical current. The measured current is directly proportional to the concentration of oxygen contained the gas mixture. But it is also sensitive to pressure changes during measurement.

The measurement method for carbon monoxide, carbon dioxide and methane is based on infrared technique. The adsorbed infrared radiation (IR) from the flow gas is measured. The wavelength of the detected peaks is unique for every gas type; the amount of adsorbed IR radiation is proportional to the amount of this gas type.

2.3 I-graphite material from the Merlin material test reactor

Figure 3 shows the research reactor Merlin at northwest with its attachments. The research reactor Merlin was located at the area of Research Center Jülich. This research reactor was decommissioned in 1985 after twenty three years of operation. Delominsition of the plant began in 1996 and was completed in 2009. Merlin was a light water moderated and cooled swimming pool reactor with a thermal capacity of at last operating time of 10 MW. Used Fuel were 2,7 kg up to 80% enriched U-235. It was operational from 1962. This reactors main purpose was irradiated of test materials with neutrons of various energies. The Highest thermal neutron flux was 8,8 * 10^{13} cm^{-2} s^{-1}. The thermal neutron flux at the front surface of thermal column was 1-2 * 10^{10} cm^{-2} s^{-1} [10]. The fast neutron flux at the thermal column was * 10^{8} cm^{-2} s^{-1} [11].

Figure 3 Merlin research reactor at Jülich

Samples where received from the Merlin reactor in 2000, from the decommissioning the IEK-6 block of graphite from within the thermal column. The thermal column is for slowing down fast neutrons which occur at nuclear reactions sites within materials on test. Figure 4 shows a schematic of the Merlin reactor and the thermal column.

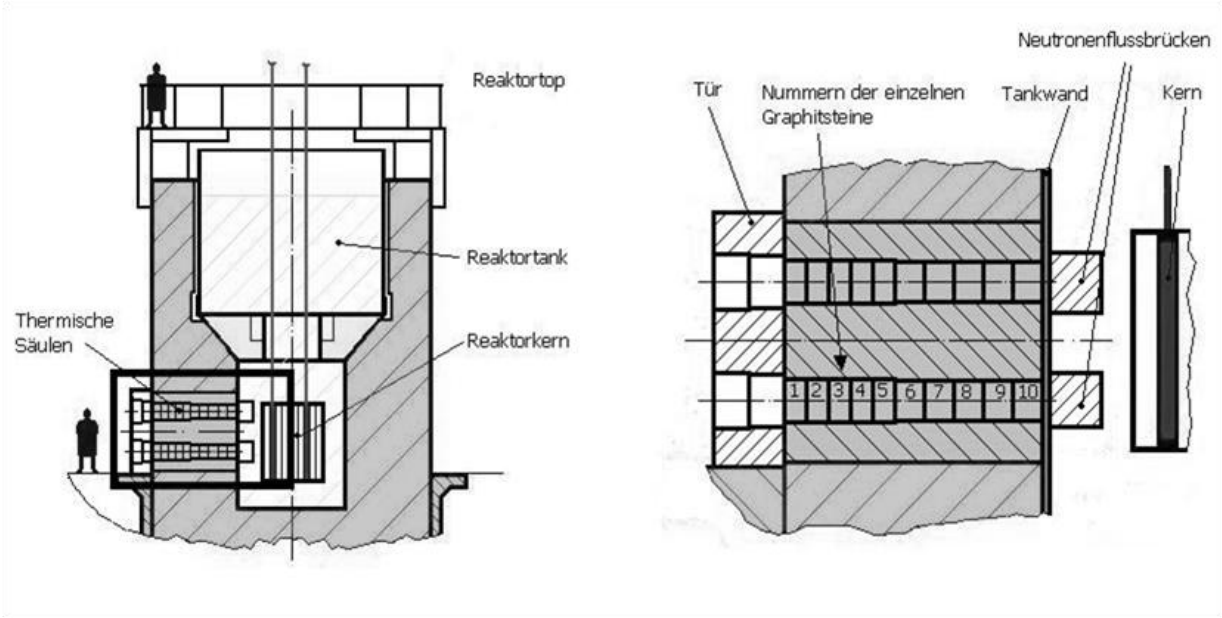

Figure 4 Schematic of the Merlin Research reactor and thermal column

2.4 Isotopic inventory in Merlin i-graphite

Samples were taken from every section graphite within reactor block and analysed using liquid scintillation counting and gamma spectroscopy. The result showed the following radionuclides where present within this i-graphite material; ^{3}H, ^{14}C, ^{60}Co,^{133}Ba, ^{152}Eu, ^{154}Eu und ^{155}Eu. Table 1 shows the measured amount of radionuclides present with Merlin i-graphite.

Table 1 Measured radionuclide inventory in Merlin i-graphite in 2000

Nuclide	Decay	Decay Product	Half life /HWZ	Concentration [Bq/g]	
				TS 10/1	TS 10/2
^{3}H	ß-	^{3}He	12,33a	4700	4760
^{14}C	ß-	^{14}N	5370a	505	449
^{55}Fe	ε	^{55}Mn	2,73a	<0,05	<0,003
^{60}Co	ß-	^{60}Ni	5,2714a	983	956
^{133}Ba	ε	^{133}Cs	10,51a	5,83	4,71
^{152}Eu	ε	^{152}Gd	13,537a	986	959
^{154}Eu	ß-/ß+ e	$^{154}Gd/^{154}Sm$	8,593a	89,8	88,3
^{155}Eu	ß-	^{155}Gd	4,76a	5,74	5,51
Total βγ				<0,003	<0,003

Unfortunately there are no virgin samples or information about manufacturing process information available for Merlin graphite. The T10 Brick was the highest contaminated sample in the thermal column, therefore samples from stone T10 were taken for further analysis. The content of tritium and radiocarbon of each numbered sample and location position in thermal column II are shown in Figure 5. The sample located nearest to the core shows the highest amount of activity.

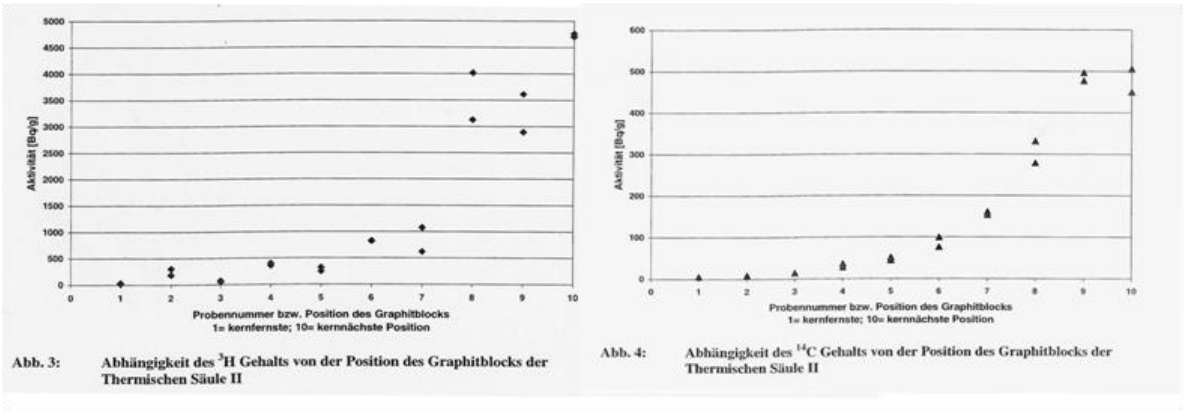

Figure 5 ^{3}H and ^{14}C content versus position in Merlin thermal column II.

2.5 Saint Laurent A 2 Graphite

2.5.1.1 General considerations about UNGG reactors

UNGG (Uranium Naturel Graphite Gaz) reactors were graphite moderated, cooled by carbon dioxide and fuelled with natural metallic uranium. EDF (Electricite De France) operated in France six gas-cooled reactors, all of which have been shutdown now for at least fifteen years.

The design of UNGG reactors is, in its general principle, very close to that of the British Magnox reactors, that was developed independently at the same period in United Kingdom. In the absence of uranium enrichment, graphite was used as a moderating material with a very high level of purity due to the necessity of the highest transparency to neutrons. Graphite has been also chosen as a mechanical support of the fuel cartridges (graphite sleeves) and as a biological shield in some reactors. A scheme of the main possible uses of graphite in UNGG reactors is shown in figure 6. The irradiated graphite from the pile or from the biological shield still lies in the reactors. The graphite sleeves that are not already shipped to the final repository are stored in silos.

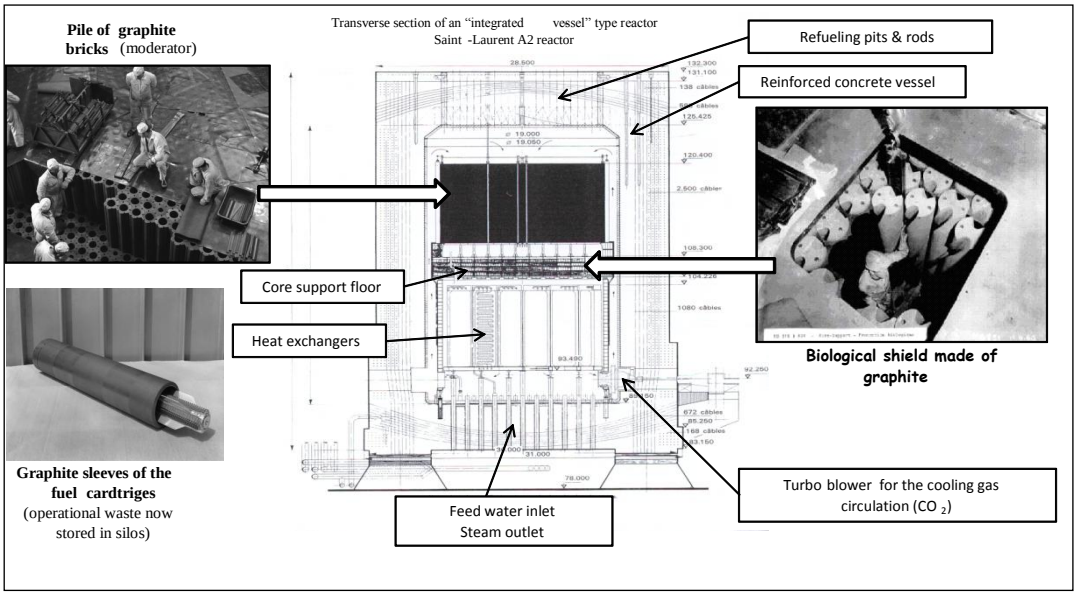

Figure 6 Uses of graphite in EDF UNGG reactors; different designs were developed, in this scheme an "integrated vessel" type reactor is presented (approximate external dimensions: 50 m height / 28.5 m diameter)

2.5.1.2 Saint-Laurent A2 reactor short history

The Saint-Laurent A2 (SLA2) reactor was commissioned in August 1971. The pressure vessel of this reactor is built of pre-stressed concrete which also acts as biological shielding. The coolant is CO_2 which circulates from top to bottom at a pressure of 29 bar in the space between the graphite and the Mg-Zr alloy fuel cladding. The operating temperature ranges between 240°C (top) and 470°C (bottom). The thermal power is 1,700 MW. The gross electrical power is 530 MWe and the net electrical power in nominal operation is 515 MWe. The thermal neutron flux (from 10^{-5} eV to 0.5 eV) in the central zone of the core and in the maximum flux plane is 3.12 10^{13} $n.cm^{-2}.s^{-1}$.

It should also be noted that this reactor was shut down between March 1980 and September 1982 following an incident which led to the melting of two fuel elements at the bottom of the F5 M19 C14 channel (loss of cooling of the channel as a result of its obstruction by a metal plate, leading to overheating of the fuel elements).

The SLA2 reactor was finally shutdown on May 25, 1992. It was operated during 11 years full equivalent operating power. It has been defueled and has been placed in a safe enclosure mode (ventilated by air with a moisture content limited to 50 %) until the final dismantling is performed.

EDF received the authorization to fully dismantle the SLA2 reactor by decree 2012-510 of May 18, 2010. All non nuclear parts of SLA2 nuclear unit have been dismantled (dismantling IAEA level II achieved - figure 2). Up to now, final dismantling (level III) is planned by 2030-2040.

Figure 7 Saint-Laurent A1 (left) and Saint-Laurent A2 (right) UNGG reactors (current state 2012)

2.5.1.3 Graphite stack description

The graphite stack of the SLA2 reactor has the form of a cylinder with a vertical axis 15.73 meters in diameter (13.43 meters of moderator surrounded by a 1.15 m thick reflector) and 10.2 meters high. The total mass of graphite is 2,440 tons including 1,580 tons of moderator and 860 tons of reflector (figure 8).

The stack's network of graphite bricks is a hexagonal mesh with a pitch of 225.16 mm. The elementary graphite blocks are prismatic bars with a hexagonal base whose distance between two opposite faces is equivalent to the network mesh. The side-by-side juxtaposition of 4,429 bars forms a bed, the SLA2 stack consisting of 8 superimposed beds (bed No. 1 is that at the bottom of the stack). Thus, the bars are superimposed and the stack may also be regarded as the juxtaposition of 4,429 columns. The graphite stack comprises:

- The lateral reflector consisting only of 828 solid columns surrounding the core
- The moderator (or core) consisting of 3,601 columns: 345 solid columns, 181 bored to 84 mm for the control rods and 3,075 columns bored to 140 mm (basically for the fuel elements)

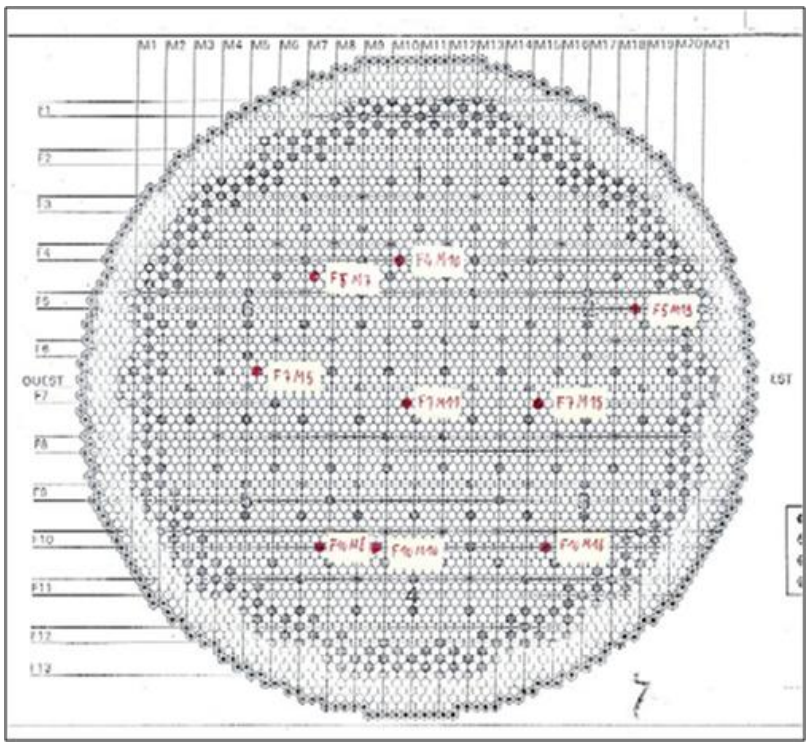

Figure 8 Section through the graphite stack of the Saint-Laurent A2 reactor - Juelich graphite cores were sampled from the F4M10 (hexagonal cell) C19 (fuel channel).

2.5.1.4 SLA2 Graphite

The graphite of SLA2 stack was manufactured by the Pechiney/SERS Company between May 1966 and November 1967. This graphite was made from Lima coke, underwent one impregnation and was purified using MgF2. During its manufacture it was tested particularly with regard to effective cross-sections, density measurements and other properties described in table 2.

Table 2 Properties of SL2 Graphite

Ashes (ppm)	B (ppm)	Li (ppm)	Co (ppm)	Cl (ppm)	Thermal neutron absorption cross section (mbarn)	density
98	0.11	0.07	0.05	-	3.76	1.68

Concerning radionuclide inventory of the irradiated SLA2 graphite from the pile, it has been determined as described in CARBOWASTE report T-3.4.3 and corresponds to the following values for the main radionuclide of interest listed in table 3.

Table 3 Isotopic inventory for SLA2 Graphite

^{3}H	^{10}Be	^{14}C	^{36}Cl	^{41}Ca	^{60}Co	^{63}Ni	^{137}Cs
$8.9\ 10^{4}$	19.1	$7.7\ 10^{4}$	37.9	83.7	$4.0\ 10^{3}$	$3.5\ 10^{4}$	47.0

The values in table 3 are in Bq / g and related to January 2017. They take no account of the influence of leaching phenomena of the underwater dismantling process. They are over-estimated mean values as described in Carbowaste report T-3.4.3.

The radionuclide inventory for cesium 137, a trace element for the fission reactions, shows that the decontamination operations adopted following the fuel element melting have been effective. In fact, this incident has no detectable effects in terms of contamination of the graphite. The levels of cesium 137 are equivalent in all the EDF reactors whether fusion of fuel elements has occurred or not. The presence of cesium 137 in very low quantities and the heavy nuclei produced are explained by the fission of traces of uranium present in the original graphite. These traces were identified in the analyses performed on the graphite at the time of their manufacture and now evidenced by the identification calculation-measurement method used for the radionuclide inventory assessment.

2.5.1.5 Core sampling

The SLA2 reactor stack was subjected to core drilling in 2005 during which 180 cores were extracted. Remote controlled tools introduced into the fuel channels of the stack were used. This technique is the same to the technique implemented for monitoring the wear of the graphite during operation. The remote-control tool (figure 4) was introduced from accesses through the refuelling pits at the top of the reactor into the channels, and performed coring on either side of the graphite bricks (figure 5) in the direction perpendicular to the channels with a diameter of about 20 mm.

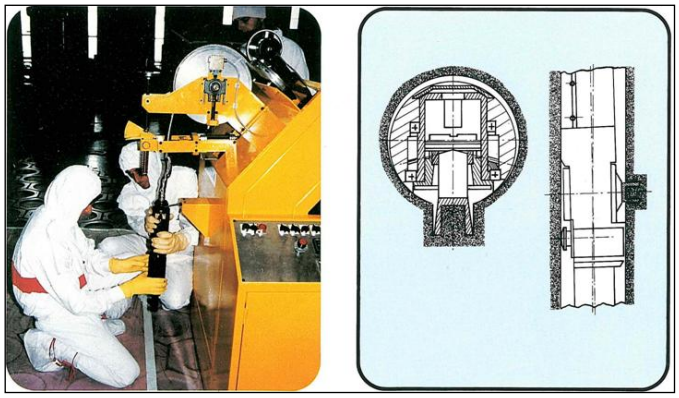

Figure 9 Remote controlled tool used for graphite stack sampling in UNGG reactors

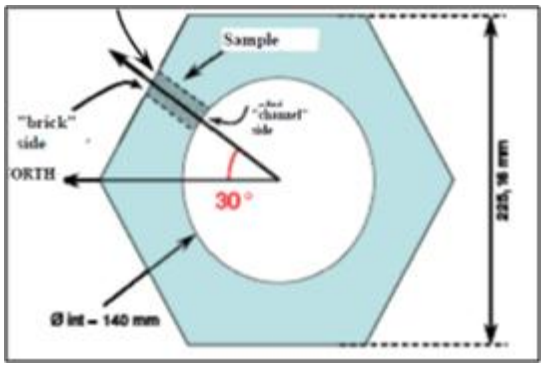

Figure 10 Schematic view of coring in a graphite brick

2.5.1.6 Samples send to FZ-Juelich

Five Samples were sent to Juelich coming from F4M10 cell C19 channel. They were chosen as being distributed over the height of the fuel channel in order to correspond to the operating temperature range in SLA2 reactor, as shown in table 4.

Table 4 Samples send to Research center Jülich

Adress	Height	Temperature °C	dose rate µSv/h	Mass sample (g)
F4M10C19	1680	443	185	17,5
F4M10C19	2460	446	193	22
F4M10C19	5120	391	462	20,5
F4M10C19	7880	294	107	20,5
F4M10C19	9260	258	9	23

2.6 Experimental results FZJ

Two kinds of thermal treatment with oxygen tests were carried out. A ceramic tube furnace with sample inserting at 1300°C was the used procedure. At first, tests, planned as inert gas tests according to M. Florjans[12] work, cold samples was moved at reached temperature from the ambient into the heating zone at 1300°C. The comparison with other experiments show, that mass losses in the range of 0,9 % were too high for inert gas tests and it with blank tests it got visible that there was no possibility to get the equipment air tight after open it in a hot state. Also by opening the equipment and placing the sample in the heating zone a lot of oxygen was ingressing into the reaction zone so that the concentration of CO and CO_2 show a peak in the beginning of the test from the incineration of graphite at the sample surface. The table 5 show results of first tests, the graphs in figures 11 and 12 show the measured CO, CO_2 and O_2 -Concentration. Because of no flushing the equipment with nitrogen the night before and pressure instabilities there was no reliable oxygen measurement possible.

Table 5 Results of radionuclide release and weight loss (weighed) after testing in ceramic tube at 1300°

Sample type	testing time [h]	3H Release [%]	14C Release [%]	Mass loss [%]	Start mass [g]
SLA 2	10,5	65,2	2,0	0,91	3,5328
MERLIN	10	93,6	5,9	0,89	3,4837

The figure 11 shows oxygen decrease in dependence of sample taking. These intial experiments highlighted the problems with the oxygen detection:

1.) The measurement method is very sensitive to pressure changes.
2.) You have to make a “zero state” calibration with a stable oxygen content (“zero-content” of oxygen)

It was not possible at this time (initial experiments) without flushing for a sufficient length of time, therefore following experiments carried out flushing overnight was done prior to the experimental test.

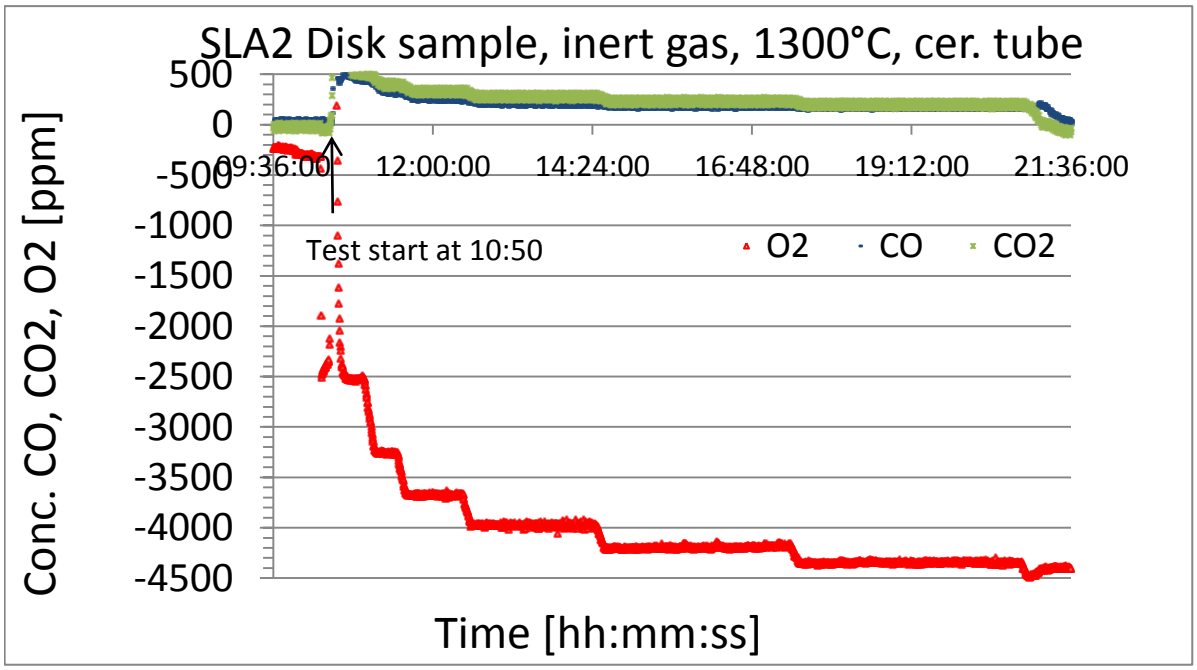

Figure 11 CO, CO_2 and O_2 values in dependence of the test time, sample: SLA 2 graphite at 1300°C in a ceramic tube, cold sample placed in a hot oven, with no flushing

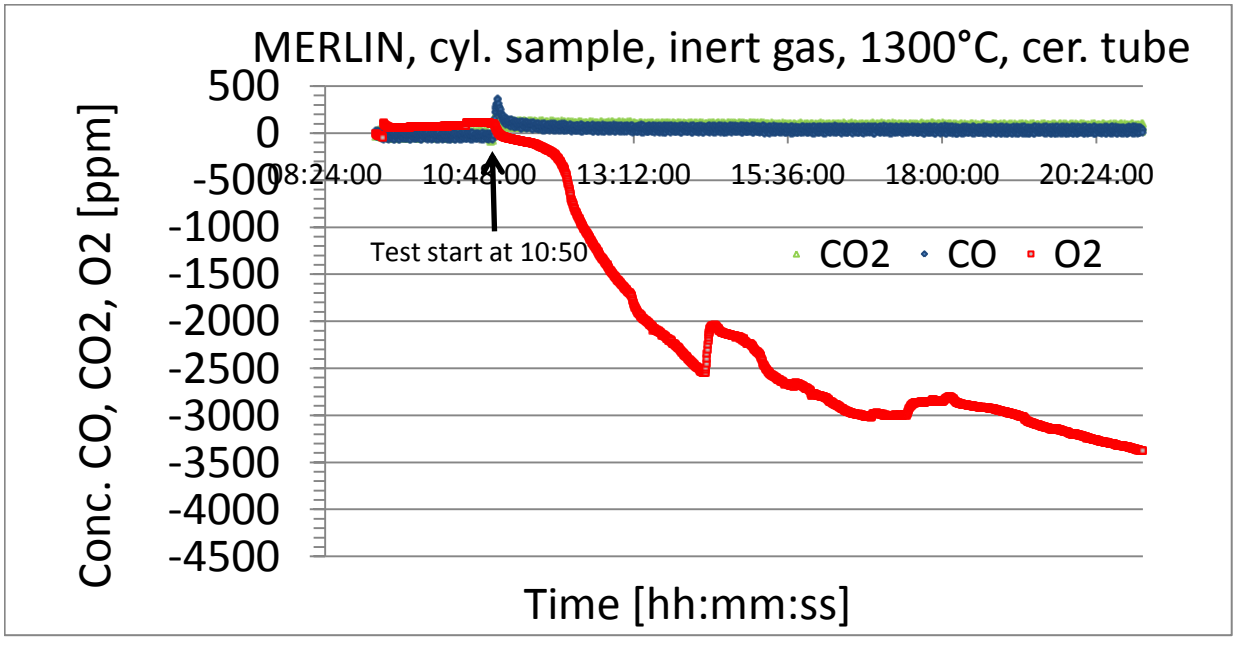

Figure 12 CO, CO2 and O2 values in dependence of the test time, sample: MERLIN graphite at 1300°C in a ceramic tube, cold sample placed in a hot oven, no flushing

Although the oxygen content of these two tests was not to detect reliably under these test conditions, the mass loss of the samples is similar. The fractional release of tritium is 95% for MERLIN graphite and 65 % for SLA 2 graphite at a mass loss at about 0,9% and the fractional release for radiocarbon is 7,5% for MERLIN graphite and 2,1 % for SLA 2 graphite after about 10 hours.

Figure 13 shows the concentrations of O_2, CO and CO_2 of a special test according to a crack in a connection piece between furnace tube and first washing bottle after closing the facility. The crack did not influence the gas flow visible as reducing of bubbles in washing bottles, but the CO-content was extremely high in the first half of the test.

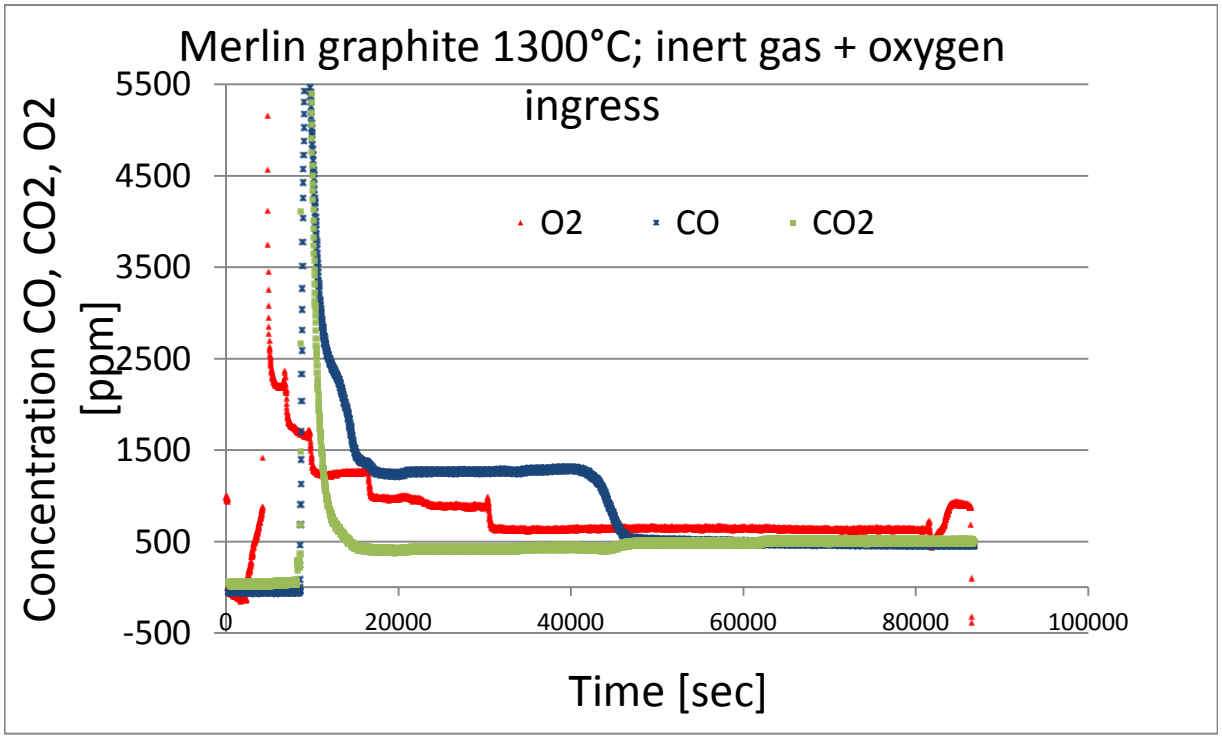

Figure 13 CO, CO_2 and O_2 values dependant on length of test, sample used was MERLIN graphite at 1300°C in a ceramic tube, cold sample placed in a hot oven, flushing was carried out before; glass cracking after sample inserting

After these two tests flushing was established to monitor oxygen content as a semi-quantitative (because of pressure change during sample inserting and liquid taking at defined times) run during the test. The CO and CO_2 peak in the figures 11-13 show the corrosion products of the sample with the remaining and /or ingressed oxygen leading to sample inserting. Comparing Figures 11 - 12 to Figure 13 it becomes visible

that there is more graphite mass loss at the test with the glass crack because the increase of the CO and CO_2-peak at the beginning of the test such as shown in Figure13.

Table 6 Shows the result s and the conditions of Merlin test with oxygen ingress through glass cracking

Sample type	testing time [h]	3H Release [%]	14C Release [%]	Mass loss [%]	Start mass [g]
Merlin	21	96,9	10,7	5,12	1,9927

The figure 14 and 15 show the percentage of tritium and radiocarbon release against treatment time.

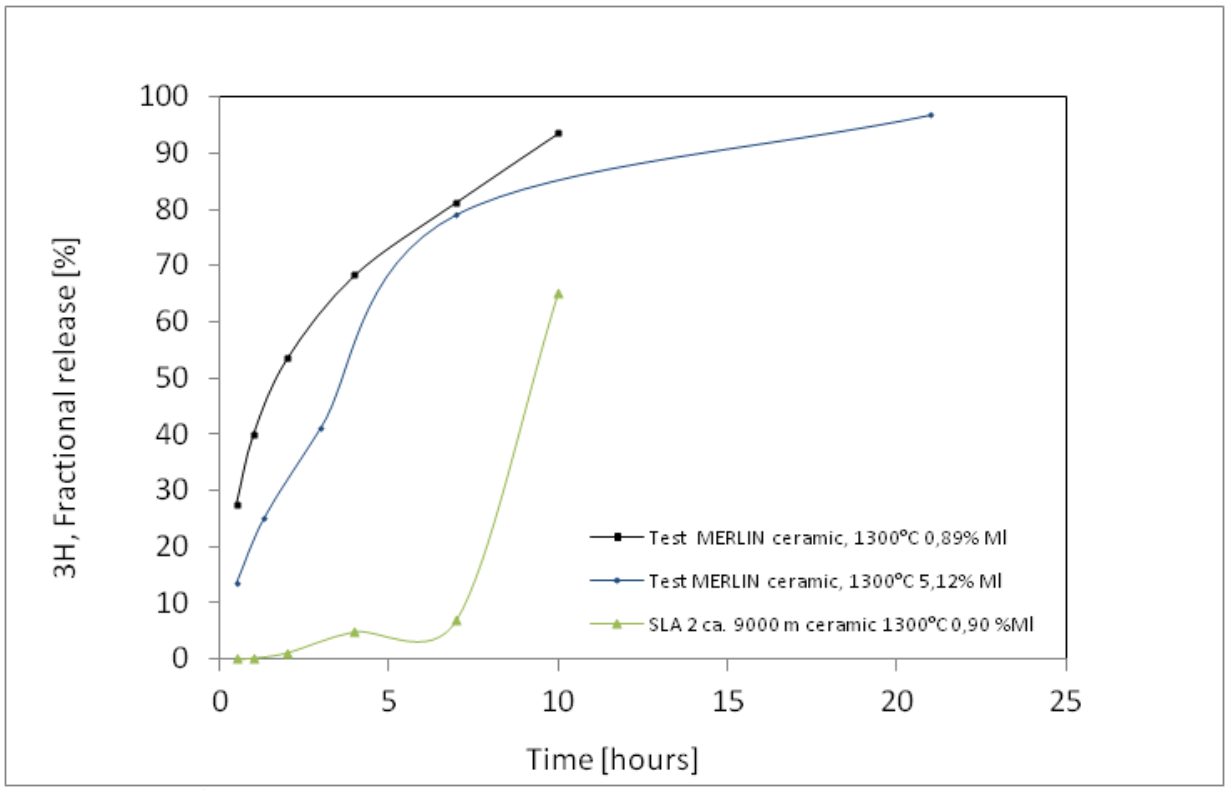

Figure 14 ^{3}H release from graphite bulk samples in nitrogen, ceramic tube

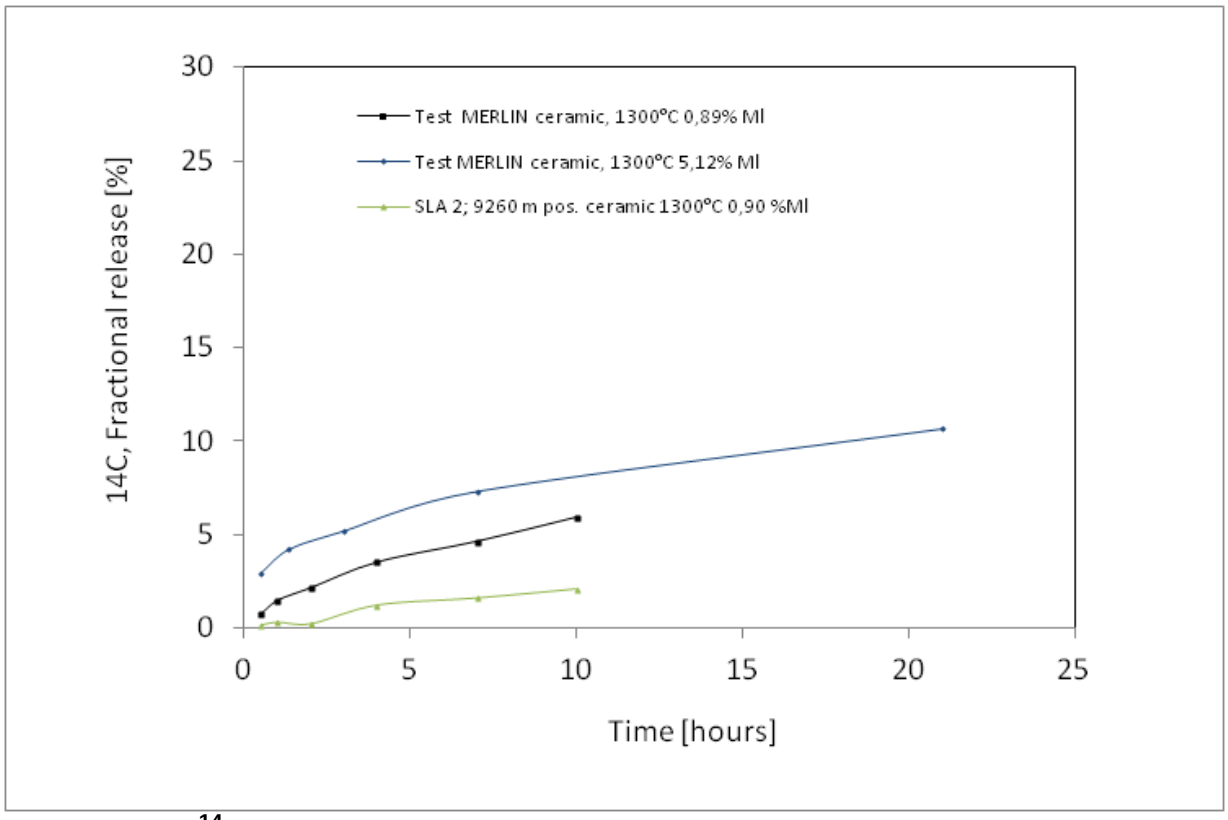

Figure 15 ^{14}C release from graphite bulk samples in nitrogen, ceramic tube

Ceramic tube treatment, the sample was inserted at room temperature and heated to 1300°C in controlled oxygen content in flow.

To limit the fluctuation of oxygen during the test for oxygen tests flow gas with 0,1% oxygen and flow gas with 0,3 % oxygen was used for tests in quartz tube. The sample was inserted in the tube, closed, flushed with flow gas for several hours and then heating was started. At quartz tube tests the temperature was limited to 1100°C. Tests with defined oxygen content in flow gas were carried out at 900°C and 750°C.

Figures 16 and 17 show the results of released tritium and radiocarbon oriented to the estimated values given at table 7.

The radiocarbon release of “Magnox quartz, 900°C, 0,1% O_2 and 0,7% Mass loss” shows a release of radiocarbon of 100%. It is supposed that this was a sample with very high contamination of radiocarbon so that the estimated value calculated from former incinerated samples of this type of graphite does not match here.

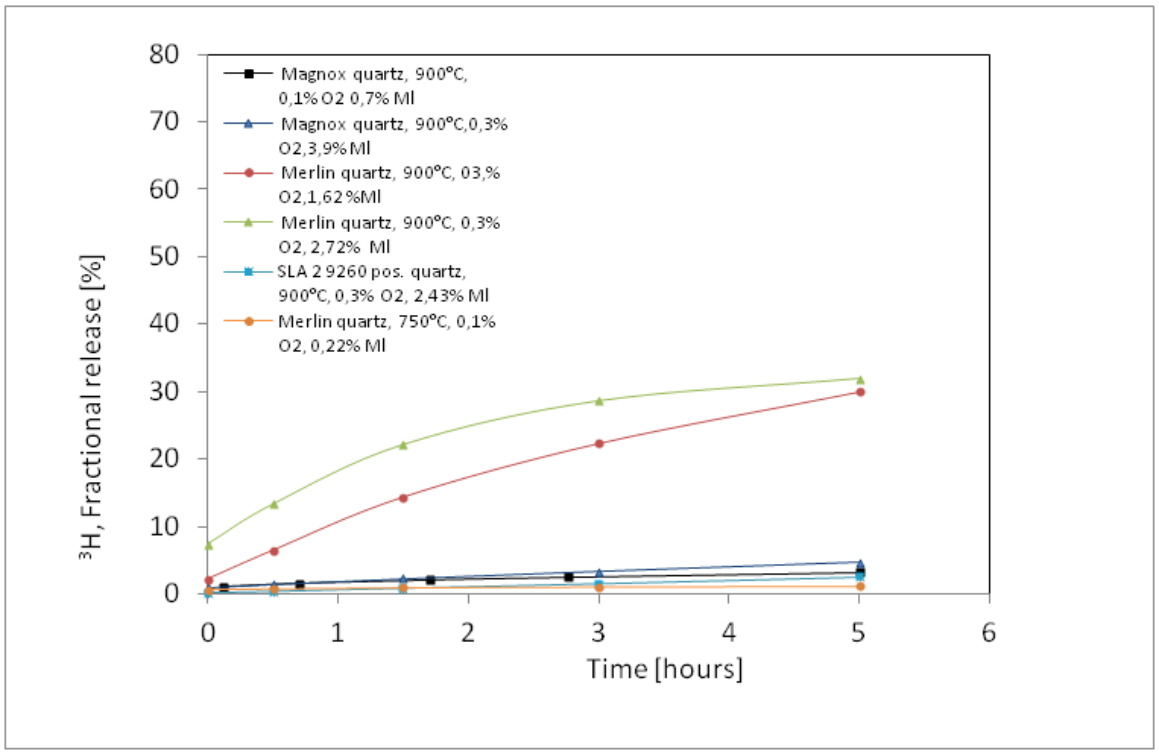

Figure 16 ^{3}H **release from graphite bulk samples in nitrogen, quartz tube**

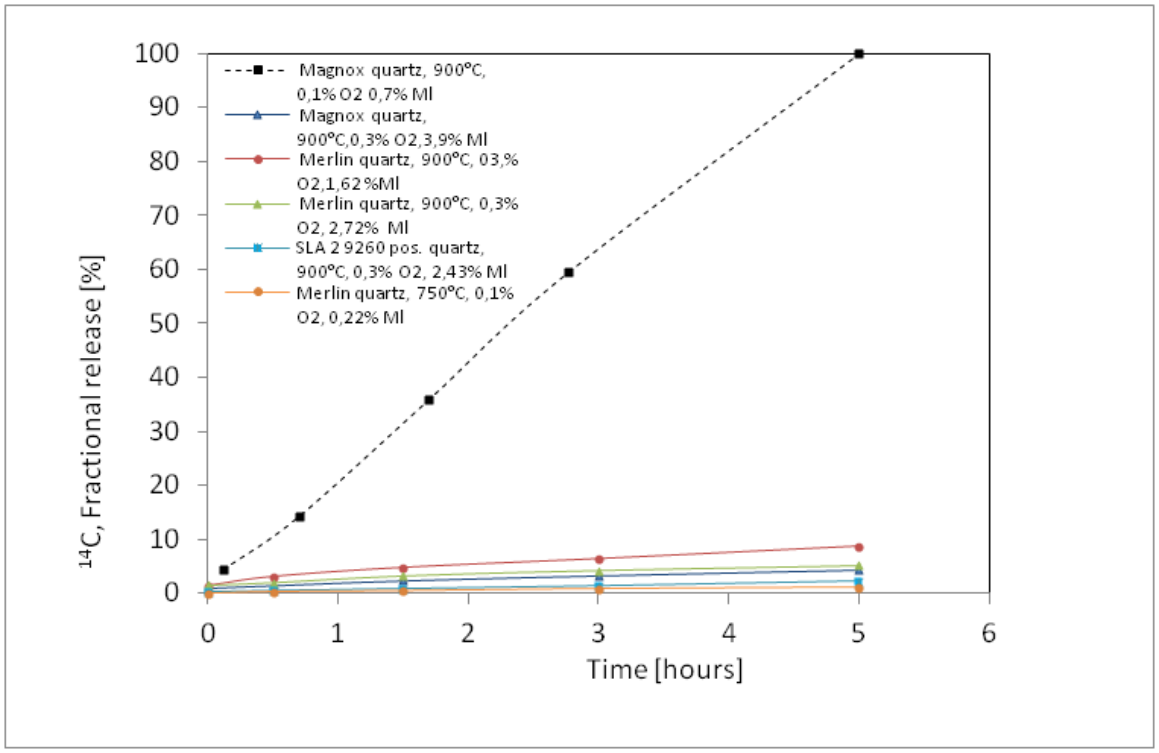

Figure 17 ^{14}C **release from graphite bulk samples in nitrogen, quartz tube**

The results of remaining radiocarbon and tritium are not available yet because radiocarbon and tritium can only be determined in a capturing solution after incinerating the sample. But characterization after treatment is not finished. Therefore determination of for the real inventory of every sample is not available. Instead of real Inventory an average inventory from incinerated samples is calculated for an estimation of radiocarbon and tritium release. Estimated activity before thermal treatment for following samples is shown in table 7.

Table 7 Estimated activities for treated samples

	Radiocarbon [Bq/g]	**Tritium [Bq/g]**
Merlin	2.47×10^2	1.83×10^2
Magnox	4.49×10^4	4.41×10^4
SLA 2 9260 h	7.73×10^4	1.54×10^4

The SEM pictures in figures 18 and 19 are taken from a virgin graphite samples from the same position before and after treatment. It is visible from comparison between these two images that treatment changes have affected surface of the graphite. The graphite layers seem to be softened during the treatment process; smaller regions are just no longer visible. Some small particles are visible at the treated graphite surface there appear to be a possibility of residue carbon deposit forming at the surface, the author considers a possible diffusion mechanism as an explanation of this change in the graphite surface structure.

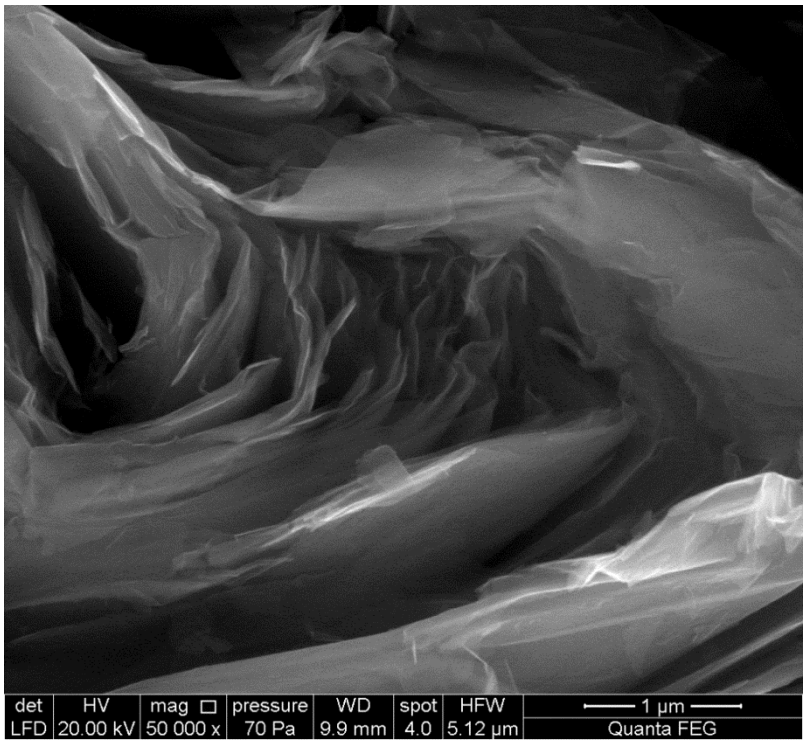

Figure 18 Virgin graphite surface before thermal treatment

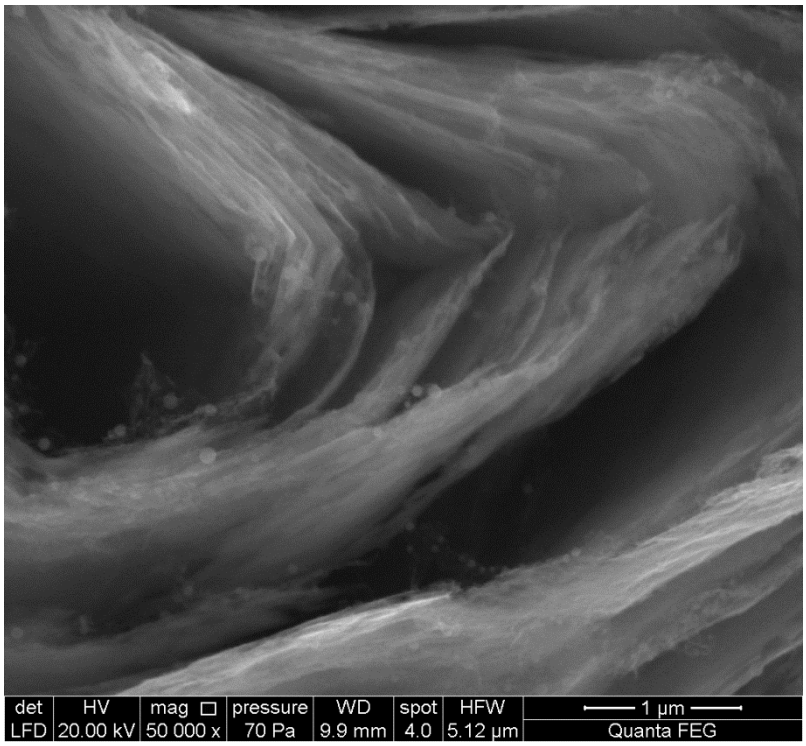

Figure 19 Virgin graphite surface after thermal treatment

2.7 Thermal treatment parameters

Parameters which proved the most successful for analytical research were using the quartz tube inlay, inserting sample, flushing with carrier gas for about 14 hours overnight and heating the closed system to test temperature to control the oxygen in the test tube. Carrier gas was nitrogen with an oxygen content ranging from 1% to 0.1%. The oxygen supply could be stabilized this way and constant for the whole test. These tests were not so effective in radionuclide release than intial experiments as oxygen ingress was not controllable but they gave greater confidence in the data achieved.

Parameters which removed the largest amount of tritium was at a temperature of1300°C and inserting cold samples into a the hot oven. Oxygen is given by sample insertion and after sample inserting the oxygen content is reduced by flushing the reaction zone with inert carrier gas (about 100-1000 ppm of ingressed oxygen present). The amount of oxygen cannot be determined sufficiently because the oxygen measurement equipment is extremely pressure dependent and measurement inaccuracy is high. Regarding experiments where Merlin samples achieved over 90% tritium removal the test was in furnace with a ceramic tube inlay and inserting cold samples into the hot oven.

For the removal of radiocarbon constant oxygen content in carrier gas proved even more effective, Merlin samples we reached highest ^{14}C releases ranging from 14% to 20%. This data suggest that radiocarbon release depends on inner and outer surface corrosion whereas tritium release depends on the temperature.

2.8 Conclusions from FZJ work

Thermal treatment experiments of i-graphite under gaseous conditions ranging from 0.1 to 1% oxygen maybe a useful method for conditioning i-graphite for final disposal. Results show that radionuclides can be separated from the graphite body via this technique.

Radiocarbon was released from Merlin samples up to 14 - 20 % with decontamination factors 1.19 and 1.14. Using test temperature of 1300°C more than 90% tritium from Merlin graphite (Decontamination factor: 30.4 and 15.4) and about 60% of tritium from Saint Laurent 2 graphite (Decontamination factor: 2.85) was removed.

These results lead the author of this research to conclude that radiocarbon is not homogeneously located in the graphite body; it is chemisorbed at the inner and outer surfaces at the pores of the graphite structure where nitrogen was absorbed before irradiation. Supporting this hypothesis is the data from i-graphite samples that where treated via cold placement into a hot oven which resulted in the remaining moisture from ambient air and air in the graphite pore system being heated fast and causing cracks in the pore structure which assist in releasing weaker bounded species at the inner surface, resulting in higher release rates of ^{3}H and ^{14}C.

Finial conclusions from this research are that; not all radiocarbon is volatile and knowledge gained by characterizing the nonvolatile remaining radiocarbon in i-graphite post treatment would assist with further supporting contributions for an i-graphite waste management strategy.

3 UoM

In collaboration with the experimental work carried out at FZJ, UoM have performed thermal treatment experiments in inert and 1% oxygen gas environments on Oldbury i-graphite.

3.1 Experimental Program

The Furnace is set up at UoM is depicted in Figure 20 which shows where the copper catalyst is located in relation to the sample zone and off gas bubbler collection. This furnace is calibrated for efficiency every five runs using ^{3}H and ^{14}C labelled sucrose standards, this process is named the recovery check. A new copper catalyst is installed when the recovery check falls below 70% efficiency or if the background collected during a blank analysis is too high. The combustion tube can then be rinsed with 4M HCl to remove any unwanted historic isotopes that may remain inside the tube prior to a new catalyst being oxidised.

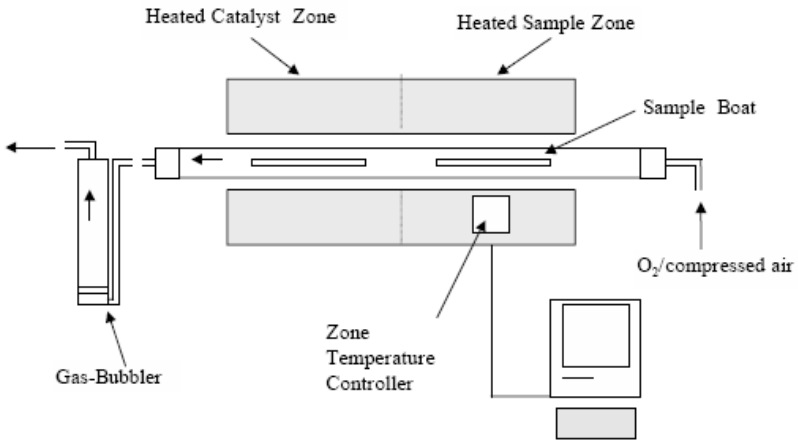

Figure 20 Schematic representation of combustion furnace used during this project

The CuO catalyst ensures all hydrogen and carbon species passing over it are converted into HTO and carbon dioxide. The first two bubblers at the end of the furnace contain 20 mls of 0.1M Nitric Acid (HNO_3) used for trapping ^{3}H present as

HTO, the last two bubblers 40 mls of carbon trap is used as a trapping agent for ^{14}C which is present as $^{14}CO_2$.

Within the CARBOWASTE i-graphite was supplied for the purpose of performing a round robin test (RRT) with 11 other laboratories taking part in work package 3. Within the isotopic requirements of this analysis was ^{14}C and ^{3}H. This analysis was performed using this technique at UoM. The results from this work and that of other CARBOWASTE partners is shown is Deliverable D-3.1.5. Good correlation was achieved at UoM providing confidence in this technique for quantification isotopic analysis of ^{14}C and ^{3}H.

The methodology followed using the carbolite® furnace is specifically designed for of ^{3}H and ^{14}C determination. This methodology is estimated to have a 10% inaccuracy associated with this process due to any gaseous losses which may occur during the analysis. The recovery checks that are performed calculate any losses which may occur during analysis allowing higher levels of accuracy to be achieved. The carbolite® furnace and LSC data of recovery check and system suitability checks are recorded and monitored over all analysis that is carried out is given below:

- ^{3}H recovery checks are typically between 80-96% recovery and quenched LSC standards 99%
- ^{14}C recovery checks are typically between 85-96% recovery and quenched LSC standards 100%
- <1% carryover between bubblers
- All bubblers are analysed to ensure all isotopic activity is captured
- All measured volumes are weighed on 4 decimal palace balance providing high levels are accuracy
- A flush is performed at the end of each analysis to ensure no carryover occurs between runs

3.2 Oldbury Graphite

The Oldbury nuclear power station consists of two Magnox class reactors; reactor 1 was connected to the electricity grid on 07/11/67 and reactor 2 on 06/04/67. Reactor 1 was shutdown on 29/02/12 and reactor 2 on 30/06/11 [7]. The Oldbury reactors were the first nuclear power station in the UK to have a pressure vessel made from pre-stressed concrete instead of steel. Reactor 2 had a gas outlet temperature of 365 °C and produced an average power output of 434MW during its lifetime, a reduction from the original design specification of 600MW. Reactor 2 produced 893 thermal power MW(t), the graphite was manufactured from pile grade A (PGA) graphite, weighing 2061 tonnes with a reactor graphite total of 2090 tonnes (including reflector and shield graphite).

Samples provided for CARBOWASTE research where supplied by NNL. The present information is what has been made available to the author. The samples were taken from an installed set (photograph figure 21), these were located in pot 634, position 4, which was placed in Channel S77 (BNL Channel 3) of Oldbury Reactor 2 from commissioning to June 2005.

Figure 21 Photographs of remaining installed sets samples at UoM

The Mean Core Irradiation of these installed sets is 30658 MWd/t. Dosimetry calculations have not been specifically carrier out for these samples; however a suitable reference sample from Oldbury Reactor 1 trepanned in 2004 has had full dosimetry calculations performed. On this basis the following information has been

provided as detailed in table 8.

Table 8 Irradiation conditions of Oldbury i-graphite provided by NNL

Irradiation Conditions	
Irradiation temp	543 K
Adjacent fuel dose	52827 MWd/t
DIDO equivalent dose	40.27×10^{20} n/cm^2
Calder equivalent temperature	543 K
DIDO equivalent temperature	597 K
DPA	5.28

Following the methodology as described in section 3.1 and Gamma Spectroscopy. The Oldbury i-graphite was determined to have the following isotopic inventory.

Table 9 Isotopic inventory in Oldbury installed sets determined on the 22nd Jan 2013

Isotope	**Specific Activity (Bq/g)**
^{3}H	36000 ± 10%
^{14}C	57000 ± 10 %
^{60}Co	10900 ± 7%

Figure 22 Laser confocal image of Oldbury i-graphite

3.3 Treatment Program

A treatment program was designed to determine the effects of oxygen on ^{3}H and ^{14}C release. The following experimental conditions were applied to oldbury installed sets i-graphite as detailed in table 10. Further sections in this report go on to detail the experiments carried out pre and post treatment in order to determine the porosity, structural and isotopic changes that have occurred to the i-graphite as a result of the thermal treatment.

Table 10 Oldbury installed i-graphite thermal treatment program

Sample Id	Temperature /°C	Gas	Time /Hours
OM20	700	Argon	4
OM19	700	Argon	5
OM22	700	Argon	6
OM18	700	Argon	7
OM10	700	Argon	8
OM17	700	1% O_2 in Argon	4
OM14	700	1% O_2 in Argon	5
OM16	700	1% O_2 in Argon	6
OM21	700	1% O_2 in Argon	7
OM15	700	1% O_2 in Argon	8
OM1	800	1% O_2 in Argon	4
OM2	800	1% O_2 in Argon	5
OM6	800	1% O_2 in Argon	6
OM11	800	1% O_2 in Argon	7
OM13	800	1% O_2 in Argon	8

3.4 Thermal treatment isotopic release

The experimental data produced from this research has been collected and shown on figures 23 and 24 for Tritium release and figures 25 and 26 for carbon-14. The green squares represent argon conditions, blue squares 1% O_2 in argon at 700°C and the red squares 1% O_2 in argon at 800°C. Isotopic release compared against treatment time and weight loss allows the data to be access on whether there is a preferential isotopic release over carbon-12 and also to evaluate the efficiency of extended run times.

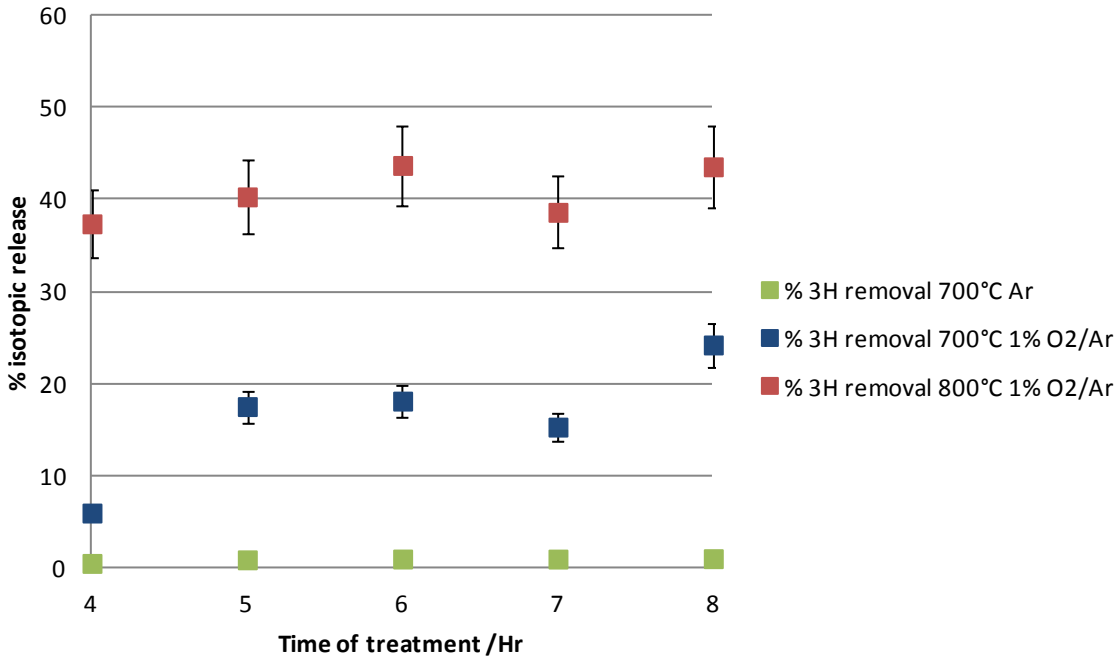

Figure 23 Tritium release versus treatment time

Under an argon environment even at extended treatment times of 8 hours <1% tritium was released. Comparing the 4 hour treatment time to the 5 hour treatment time under 700°C 1% O_2 in argon showed a significant increase in the amount of tritium released. This was under a constant flow of 1% O_2 (150 mls/min) however little difference is observed in tritium release rates between 5 hour and 8 hour treatment times. A similar trend was observed under 800°C with little difference in tritium release rates observed between 4 hour and 8 hour treatment times. The effect of temperature with tritium release is very clear from the graph in figure 23, for the additional 100°C an ~20% more tritium activity has been released.

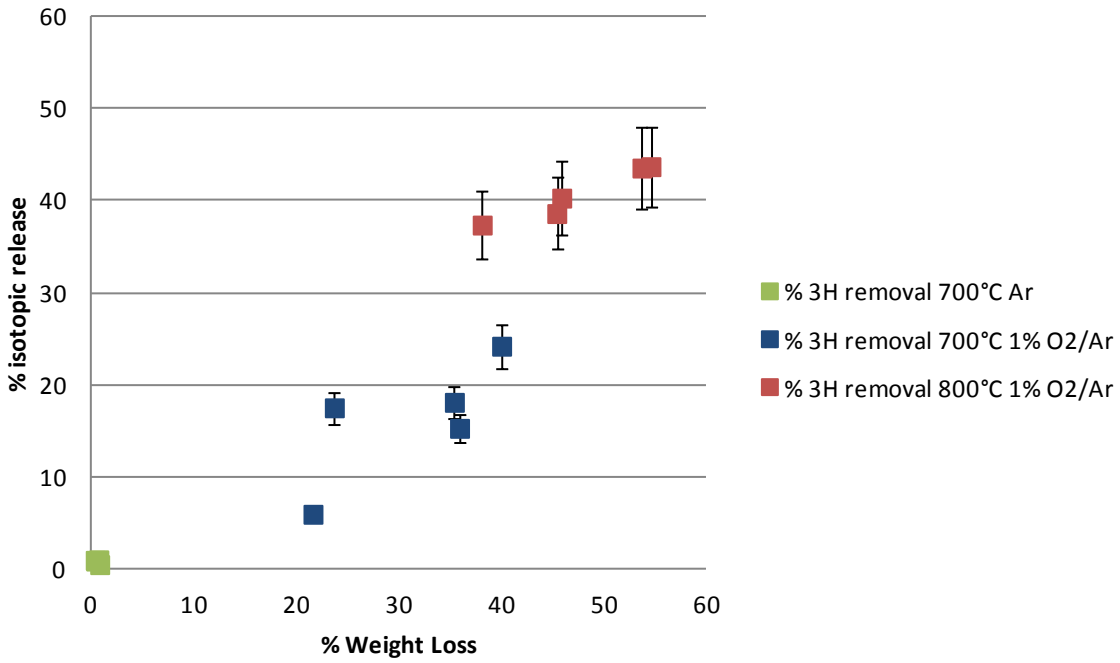

Figure 24 Tritium release versus percentage weight loss

Tritium dependence on temperature is clearly represented by this spread of data on figure 24. High levels of tritium have been release at 800°C compared to 700°C. However very little (<1% tritium) were released at 700°C under an argon environment. This direct dependence on oxygen, temperature and weight loss gives valuable insight into the behaviour of tritium and is mobility within i-graphite.

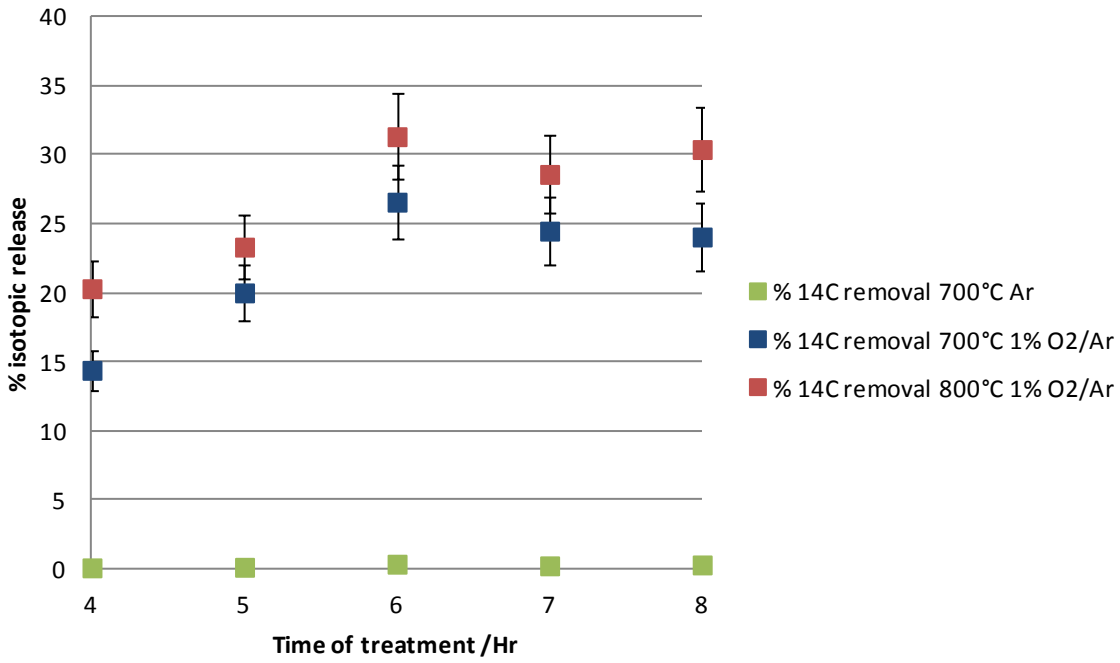

Figure 25 ^{14}C release versus treatment time

The carbon-14 release plotted against treatment time in figure 25 shows a <0.3% ^{14}C release under argon gas at 700°C for all experiments. The comparison of 700°C and 800°C show a significant agreement in ^{14}C release rates. The increased temperature appears to have little effect on the ^{14}C release, the error bars on the graphs are set at ±10% due the the limitations of the furnace used for this analysis.

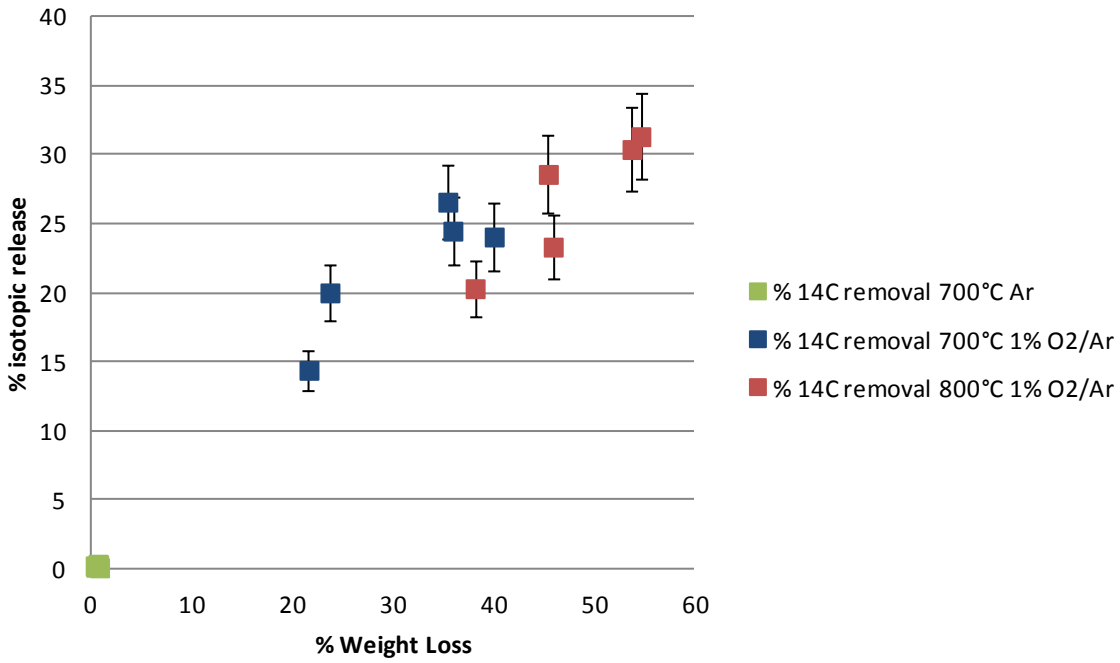

Figure 26 ^{14}C release versus percentage weight loss

The trend of ^{14}C release rate being similar for 700°C and 800°C conditions observed in figure 25 is continued with the percentage isotopic release versus percentage weight loss on figure 26. The ^{14}C released under 800°C 1% O_2 in argon treated samples reached a maximum of 31% ^{14}C with a weight loss of 54%. The ^{14}C released under 700°C 1% O_2 in argon treated samples reached a maximum of 27% ^{14}C with a weight loss of 40%. The terminology weight loss here refers to the pre and post treatment weight lost, not post irradiation. Similar trends in ^{14}C behaviour have been observed under chemical treatment research carried out as part of the CARBOWASTE research program T-4.3.3b.

3.5 Post Treatment Analysis

As can be seen in figure 27 large degradation of the sample was achieved at 800°C compared to 700°C. All samples analysed under 800°C 1% O_2 in Argon gas conditions were not further analysed on the TriStar (BET) surface area or He Pyc equipment. This is due to the almost powder consistency of the material and risk of contamination of apparatus.

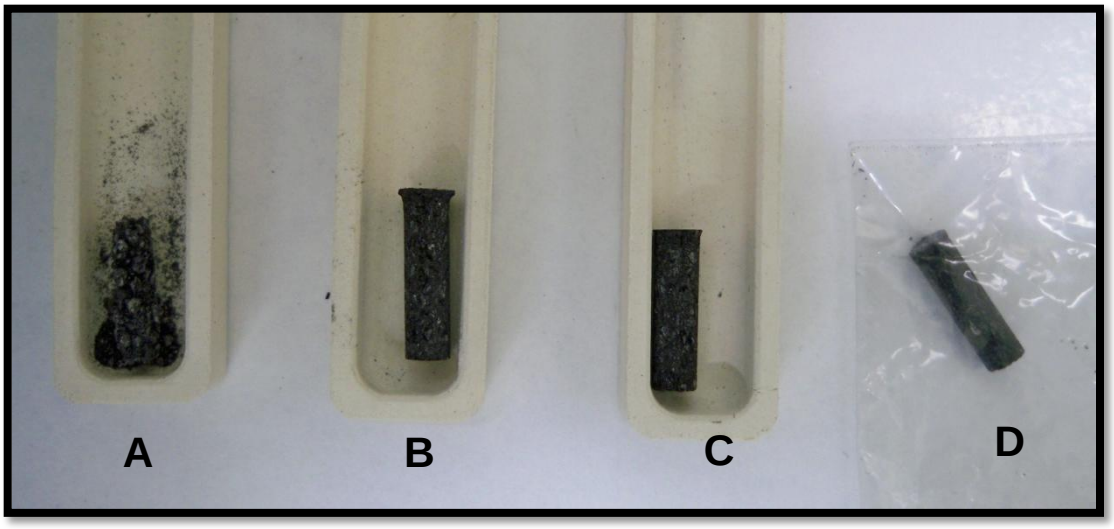

Figure 27 Comparison of i-graphite samples pre and post treatment, A = 800°C 1% O_2/Ar for 5 hours, B = 700°C 1% O_2/Ar for 5 hours, C = 700°C in Argon gas for 5 hours and D = untreated sample

Sample D in figure 27 is the untreated material, it can clearly been seen in the photograph that the effects of a 1% O_2 environment at 800°C has had on the material structure. All samples analysed at 800°C in 1% O_2 gas become heavily eroded and had a powered surface texture. This affected post thermal treatment analysis handling and unfortunately impacted on the tests that were able to carry out on these samples.

3.6 XRD

X-Ray Diffraction (XRD) provides a method of characterisation and identification of polycrystalline phases within a test specimen. Using XRD to measure the interplanar *d*-spacing between successive planes of a crystalline material, it is possible to determine values for the crystal lattice parameters.

The XRD apparatus used for this work was a Philips X-Pert Modular Powder Diffractometer (MPD), shown in Figure 28. The machine operates in a θ-2θ (Bragg-Brentano) configuration across a range from 5 to 95°2θ. A graphite monochromator and fixed copper anode X-ray source with a K_α = 1.45060 Å are used as standard with a generator setting of 45 kV, 40 mA and receiving slit of 0.2 mm. The samples were scanned as bulk solids using a continuous scan with a step size of 0.05°2θ. A standard step time of 10 s was implemented across all samples. Three samples were scanned at approximately 25°C:

- Sample OM23 – Untreated
- Sample OM20 – Treated in Ar atmosphere at 700°C for 4 hours
- Sample OM17 – Treated in 1% O_2 in argon atmosphere at 700°C for 4 hours

Figure 28 Philips X-Pert Modular Powder Diffractometer

When considering X-ray diffraction, it is useful to consider the regular series of atoms within crystals as parallel planes, and an X-ray beam diffracted from these atoms as synonymous with X-ray reflections from such planes. Consider two such atomic planes *P1* and *P2*, separated by a distance *d* such as those shown in figure 29. When conducting XRD measurements, parallel incident X-rays *1* and *2* impact on planes *P1* and *P2* at an angle *θ*. Reflections *1*' and *2*' occur only if the waves they represent are in phase. This requires that the difference in path length between *1*,*1*' and *2*,*2*' is *n* wavelengths, where *n* is an integer, which is equal to twice the distance between *1* and *2*.

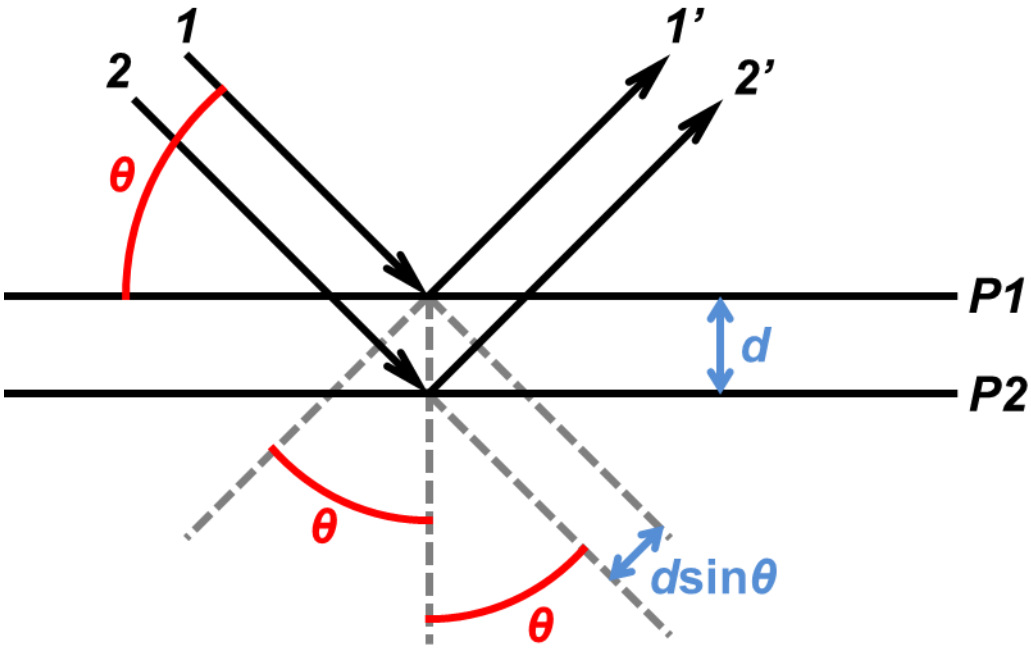

Figure 29 Schematic outlining the basic principle of X-Ray Diffraction

This phenomenon is expressed mathematically by Bragg's Law:

$$n\lambda = 2d_{hkl}\sin\theta$$

n = an integer
λ = the wavelength of the incident X-rays (1.54060 Å)
θ = the angle of the incident X-rays
d = the interplanar spacing
h, *k* and *l* are the Miller indices of a given Bragg plane

Therefore, by measuring the incident angles at which reflections are detected (i.e. where Bragg's law holds); it is possible to determine a value for *d* if *λ* is known. By rotating an X-ray source and detector pairing around a stationary sample (in this case sweeping an angle from 5-95°2θ), the XRD apparatus provides a series of peaks which can be used for determination of crystal parameters.

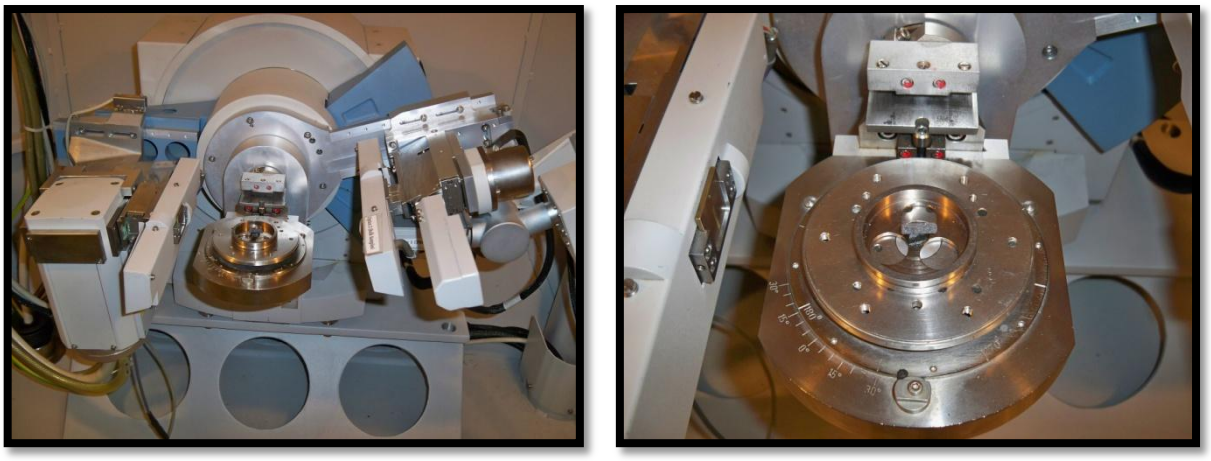

Figure 30 Goniometer inside the Philips MPD with sample on the central stage

Data smoothing was not performed on the data collected during these measurements. Artificial peak broadening as an artefact of the testing apparatus is observed during scanning. Such broadening is corrected for with the use of a silicon standard specimen and subtracting the relevant machine broadening from the specimen scans. Typical scan results on nuclear grade graphite over this angle produce a nine-peak list which is well demonstrated in the Inorganic Crystal Structure Database (ICSD) entry for "graphite" 00-056-0159.

The resulting spectra from the three scanned samples are shown below in figure 31. The peaks are labelled according to the plane reflections they refer to. The vertical axes have been normalised to the (0002) peak.

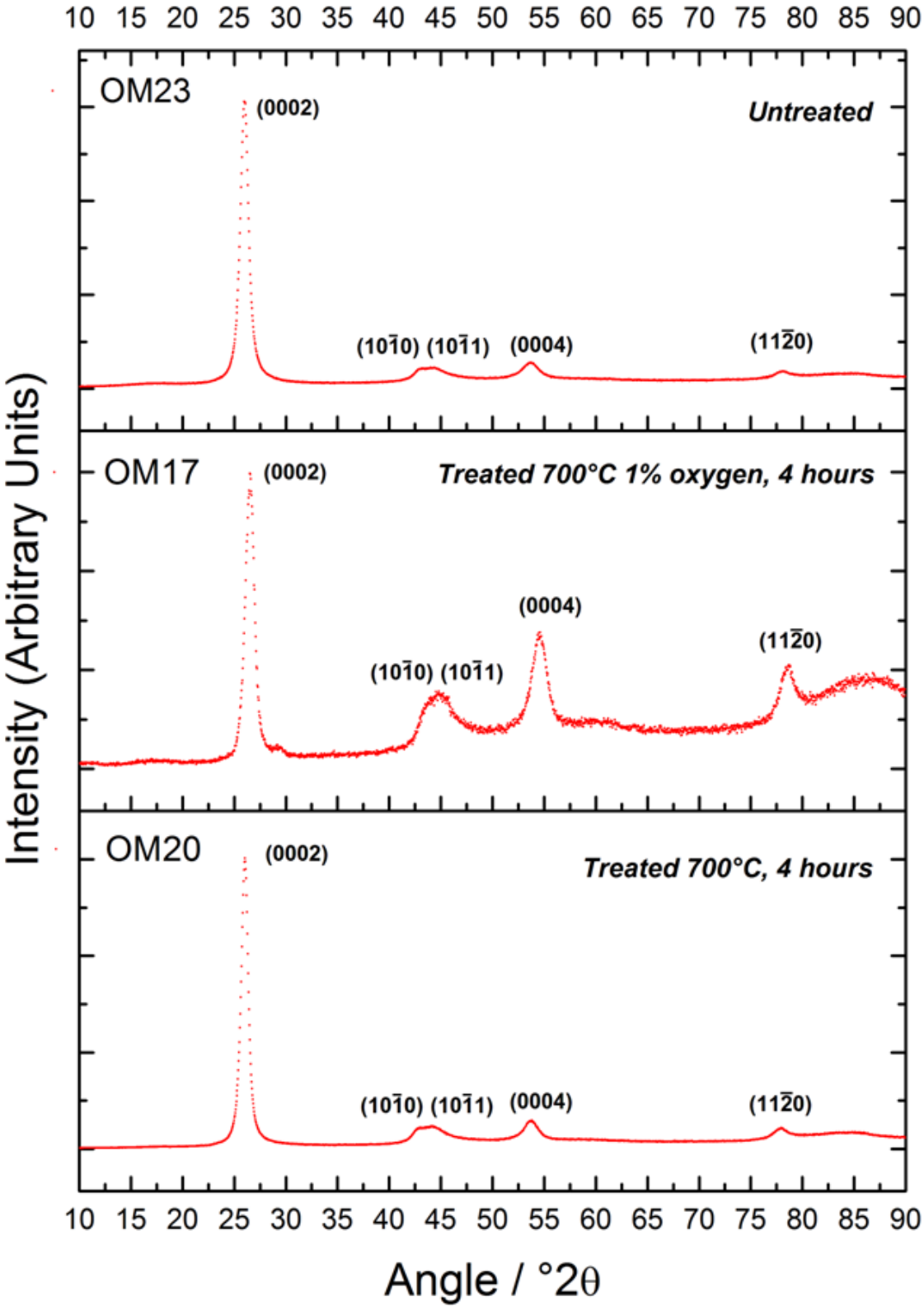

Figure 31 XRD spectra for the three samples tested

Upon immediate inspection, it is clear that the difference between the spectrum from the initial untreated specimen and that of the specimen treated with 1% oxygen is far greater than between the untreated and the sample treated in pure argon (OM20). The XRD conditions were identical for each of the three specimens and the intensity of the (0002) peak fell from little over 60,000 counts for the untreated sample to 47,500 counts for the pure argon treatment and to 3,300 for the 1% oxygen treatment. The efficiency of the reflection is dependent on the density of atoms within the plane under consideration; the fact that the intensity has dropped by such an extent with the oxygen treatment suggests that the capacity of the basal planes to reflect X-rays has been reduced to a large degree.

Application of Bragg's Law to the data obtained from these three sample scans reveals a decrease in the size of the *a* and the *c* lattice parameter with treatment in 1% oxygen. Results are shown in table 11.

Table 11 Lattice parameters for test specimens

Sample	Treatment	*a* / Å	*c* / Å
OM23	Untreated	2.45	6.85
OM17	700°C, 1% oxygen for four hours	2.43	6.71
OM20	700°C, pure argon for four hours	2.45	6.83

An indication of the degree of crystallinity can be garnered from the breadth of the peaks within the spectra. Crystallite sizes L_a and L_c are inversely proportional to the breadth of the $(11\bar{2}0)$ and (0002) peaks respectively, and can be estimated using the Scherrer equation:

$$L = \frac{k_s \lambda}{\beta_\theta \cos \theta_{obs}}$$

k_s is the shape factor (0.9)

λ is the incident X-ray wavelength

θ is the Bragg angle

β_θ is the (corrected) full width at half maximum of the peak at Bragg angle θ

As with the lattice parameter calculations, the (0002) and $(11\bar{2}0)$ peaks are used. A certain degree of artificial peak broadening is observed as a result of the

diffractometer (machine broadening). This is corrected with the use of an instrumental silicon standard and:

$$\beta_\theta = \beta_{obs} - \beta_{std}$$

β_{obs} is the measured full width at half maximum

β_{std} is the standard correction value for the instrument used

Table 12 lists the crystallite size values obtained. The Scherrer equation merely provides an estimate of the crystallite size however. Taking this into consideration suggests that the treatments conducted demonstrate little to no effect on the crystallite size with respect to *a* or *c*.

Table 12 Results from application of the Scherrer equation.

Sample	Treatment	L_a / Å	L_c / Å
OM23	Untreated	42	95
OM17	700°C, 1% oxygen for four hours	53	87
OM20	700°C, pure argon for four hours	58	71

3.7 Gamma Spectroscopy

Gamma spectroscopy analysis was performed using a NaI(Tl) low resolution gamma spectrometer with a 2x2 crystal size. The detector is manufactured by Canberra, activity calculations were performed using the Genie2K software[13]. The calibration software ISOCS, also developed by Canberra was used for efficiency calibration and a ^{152}Eu source of known activity was used for energy calibration. The set-up is shown in figure 32.

Figure 32 Gamma spectroscopy analysis

The Gamma spectroscopy equipment must be calibrated before use. Two calibration stages are required: energy calibration and efficiency calibration. Energy calibration relates the channel number of the detector to a particular photon energy, this step can be performed using any standard source with known composition. For this analysis a ^{152}Eu sealed source was used. This isotope emits a wide range of photons energies and therefore provides an accurate calibration over the entire spectrum. Efficiency calibration, which relates the count rate to the activity of the source, requires a close match between calibration geometry and sample geometry. The ISOCS software package can be used to calibrate the efficiency of the detector for any sample

geometry, counting geometry and material composition[14]. The geometry of the samples was replicated using this package, as illustrated in Figure 33.

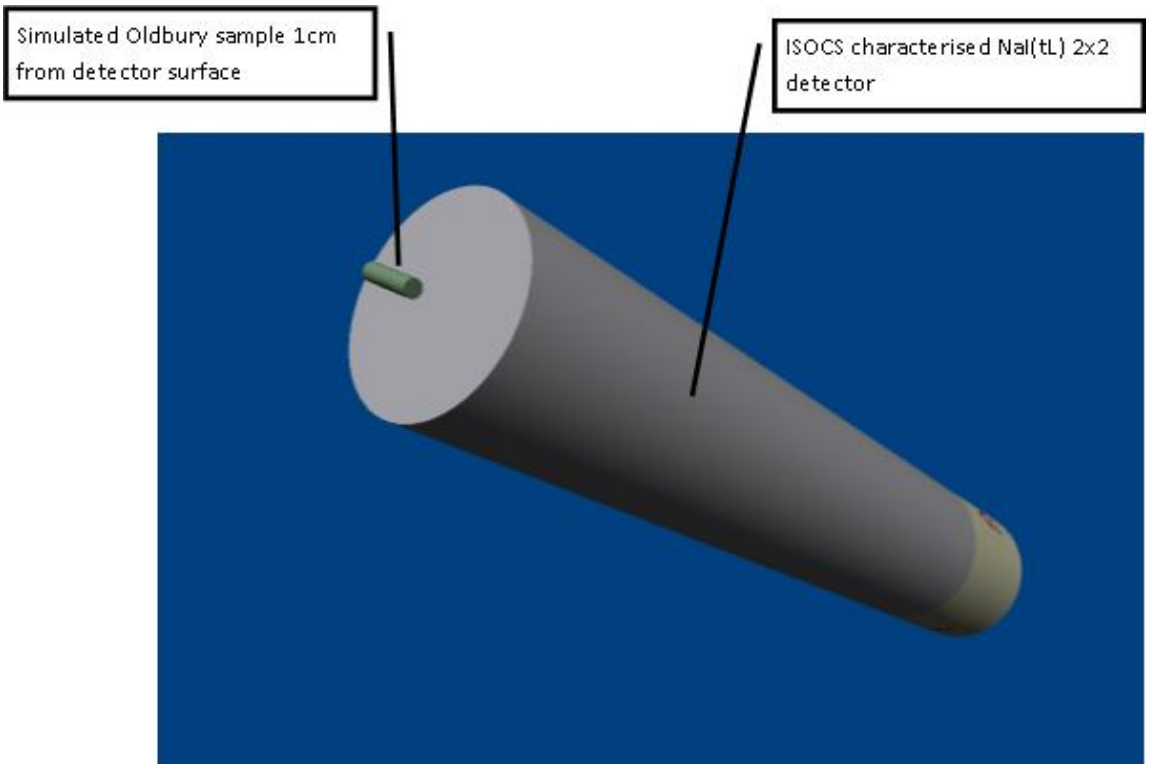

Figure 33 Screenshot from the ISOCS calibration software

All analysis was performed using the Genie2K analysis software, which also performs uncertainty analysis. The results are given in table 13.

Table 13 Activity of ^{60}Co in samples pre and post-treatment

Sample Id	Treatment Conditions	Pre treatment (kBq/g)	Post Treatment (kBq/g)	Remaining activity (%)
OM20	700°C Ar - 4 hours	9.61 ± 7.3%	9.59 ± 7.0%	99
OM19	700°C Ar - 5 hours	13.8 ± 7.5%	13.0 ± 7.3%	94
OM22	700°C Ar - 6 hours	N/A	N/A	
OM18	700°C Ar - 7 hours	12.5 ± 7.5%	12.4± 7.2%	99
OM10	700°C Ar - 8 hours	9.9 ± 7.5%	9.7 ± 7.5%	98
OM17	700°C 1% O_2/Ar - 4 hours	13.6 ± 7.2%	12.0 ± 7.5%	88
OM14	700°C 1% O_2/Ar - 5 hours	7.6 ± 7.5%	6.4 ± 7.2%	84
OM16	700°C 1% O_2/Ar - 6 hours	10.6 ± 7.3%	9.1± 7.5%	86
OM21	700°C 1% O_2/Ar - 7 hours	8.7 ± 7.5%	6.9 ± 7.2%	79
OM15	700°C 1% O_2/Ar - 8 hours	9.0 ± 7.3%	8.4 ± 7.5%	93
OM1	800°C 1% O_2/Ar - 4 hours	12.8 ± 7.5%	9.8 ± 7.1%	78
OM2	800°C 1% O_2/Ar - 5 hours	11.1 ± 7.3%	8.3 ± 7.2%	75
OM6	800°C 1% O_2/Ar - 6 hours	12.1± 7.5%	9.5 ± 7.3%	78
OM11	800°C 1% O_2/Ar - 7 hours	10.9 ± 7.1%	7.1 ± 7.5%	65
OM13	800°C 1% O_2/Ar - 8 hours	10.0 ± 7.2%	7.0 ± 7.5%	70

Experiment limitations within this analysis include:

1. Varying sample geometries; post treatment analysis was performed while sample remained in the combustion boat, altering the height position and environment of the sample
2. Weight loss changes between samples post treatment (density change)
3. Calibration was applied to both pre and post samples without weight loss alterations being applied due to time constraints

However from this crude experimental program some conclusions can be drawn, such as in inert environment of 700°C argon gas little/none of the ^{60}Co is removed and in a

similar pattern to ^{3}H and ^{14}C at 700°C in 1% oxygen in argon gas approximately ~20% of the ^{60}Co is removed. Following on from this at 800°C in 1% oxygen in argon gas approximately ~30% of the ^{60}Co was removed. This result is most unexpected as initial considerations when performing thermal treatment where that the gamma isotopes remained in the combustion boat or in the combustion tube. Following this result future analysis at UoM will consider testing the trapping agents for gamma isotopes.

3.8 Autoradiography

Autoradiography provides a visual distribution pattern of radiation present in the surface of a sample, depending on isotope energy. Autoradiography can therefore determine β and γ radiation present within a nuclear i-graphite sample with energy above 0.018MeV. Weak β-emitting particles are stopped by the coating on the phosphor storage film (which is the recording medium used for this technique). Autoradiography therefore is a qualitative technique used to analyse high energy β and γ isotopes present within a nuclear graphite sample.

There are many advantages of this technique including; a reduced exposure time compared to traditional autoradiography using X-ray film, increased sensitivity with a linear dynamic range of 1 to 100000 which allows both weak and strong energy isotopes to be analysed simultaneously in a single exposure, and the fact that phosphor storage films are reusable.

Sample size, or preferentially diameter has significant affect on the autoradiography results. High energy radionuclides have sufficient energy to pass through the graphite matrix and excite the autoradiography film being used. Lower energy radionuclide's would be hindered by a sufficiently thick piece of graphite. Autoradiography analysis of graphite samples thicker than 1cm have proved difficult to analyse with the high energy radionuclides saturating the film after only a few hours, making comparisons between graphite samples that have had varying levels of dose or exposure inconclusive.

Autoradiography analysis of Oldbury installed sets i-graphite has been performed using the Amersham 9410 selecting the red laser with a wavelength of 633nm and a pixel size of 50 microns which is appropriate to the type of film being used. Average intensity, standard deviation, variance, minimum and maximum intensity and area has then be calculated using the Amersham software. This allows the background to be deducted from the samples being analysed and highlights any discrepancies between results. Figures 34-37 show that the phosphor storage screen analysis performed pre and post thermal treatment.

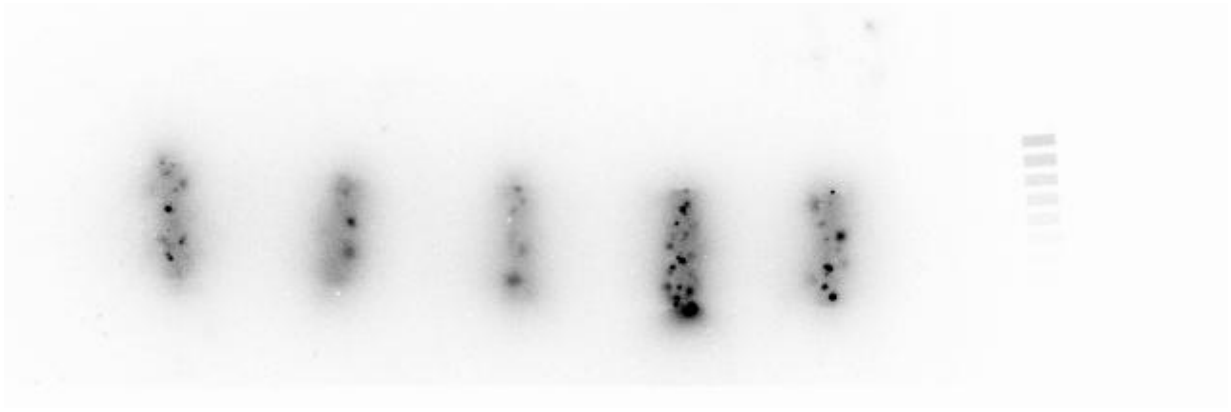

Figure 34 Autoradiography analysis of samples OM 14, 15, 16, 17 and 21

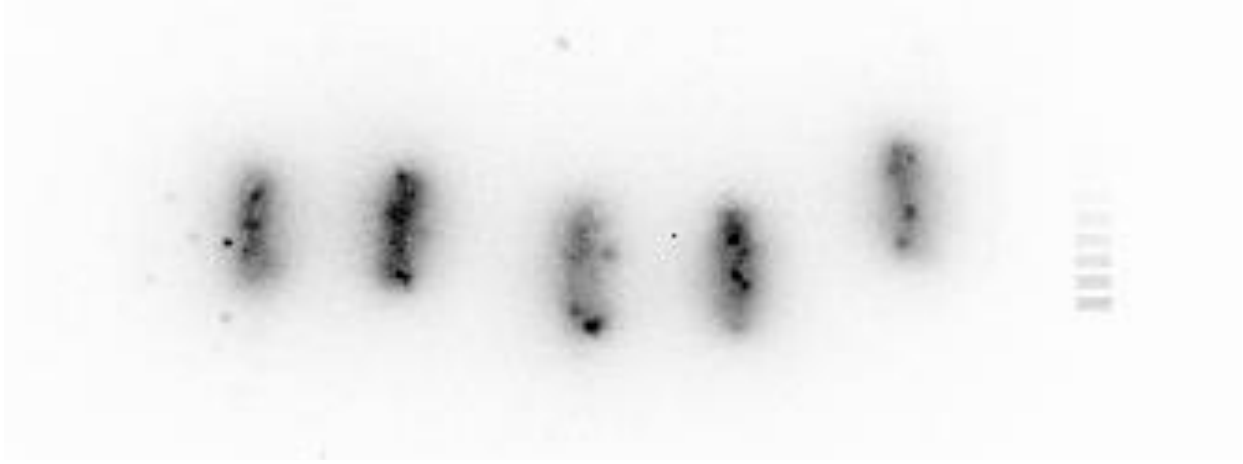

Figure 35 Post treatment 700°C 1%O_2 Autoradiography analysis of samples OM 14, 15, 16, 17 and 21

Table 14 Comparison of isotopic distribution by Autoradiography from figures 32 - 33

Sample number	Treatment time /hours	Initial results Fig. 34		Post treatment results Fig. 35	
		Average Intensity	Std Dev	Average Intensity	Std Dev
OM14	5	2363	2079	1198	608
OM15	8	3253	2083	1501	962
OM16	6	1731	612	1312	648
OM17	4	2175	779	1911	967
OM21	7	2034	1173	1454	779

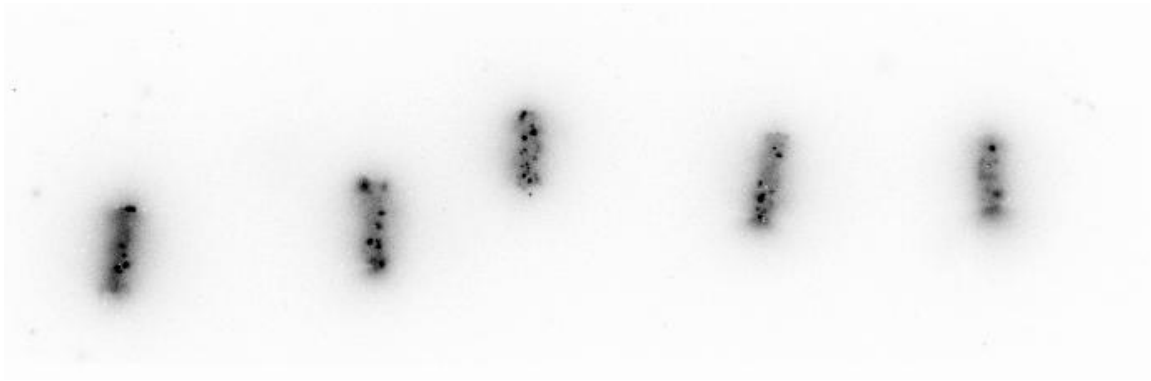

Figure 36 Autoradiography analysis of samples OM 1, 2, 6, 11 and 13

Figure 37 Post treatment 800°C 1%O_2 Autoradiography analysis of samples OM 1, 2, 6, 11 and 13

Table 15 Comparison of isotopic distribution by Autoradiography from figures 34 - 35

Sample number	Treatment time /hours	Initial results Fig. 36		Post treatment results Fig. 37	
		Average Intensity	Std Dev	Average Intensity	Std Dev
OM1	4	1265	694	803	468
OM2	5	1496	1072	854	369
OM6	6	1439	912	713	355
OM11	7	1529	885	1308	715
OM13	8	1945	1268	1288	593

Autoradiography comparison:

- Inhomogeneous distribution of activity resulting in very high standard deviation
- Orientation limitations

- Weak trends observed between treatment time and average intensity
- Overall post treatment average activity lost is in the region of 40%

3.9 Helium pycnometry

Gas pycnometry provides a method of measuring the **skeletal volume** of an irregular or porous specimen. Combined with an accurate measure of the mass of the specimen, this value can be used to determine the **open** and **closed porosity** within a porous material. The University of Manchester utilises an *AccuPyc II 1340* pycnometer analysis system alongside a *Sartorius Cubis ultramicro* balance for accurate mass determination. The *AccuPyc II 1340* is a constant volume gas pycnometer, which consists of two chambers, **A** and **B**. Chamber **A** is a calibrated chamber of known volume with a removable air-tight cap which houses the test specimen. Chamber **B** is a calibrated reference expansion chamber of known, fixed volume. A valve controls the flow of gas between the two chambers. This set-up is shown in figure 38.

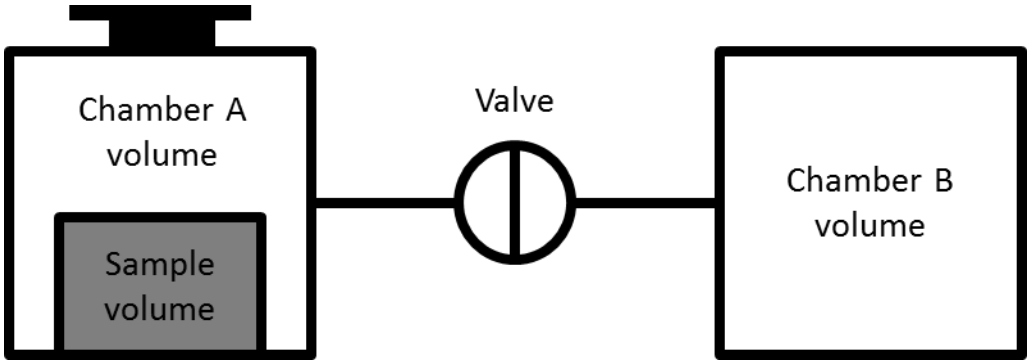

Figure 38 Schematic of a constant volume gas pycnometer

With the test specimen inserted into chamber **A**, the sample chamber is pressurised to an elevated pressure. The valve is closed so the reference chamber **B** remains at ambient pressure. Application of the ideal gas equation gives expressions for the gas within two chambers:

$$P_A(V_A + V_S) = n_A RT$$

$$\boldsymbol{P_B V_B = n_B RT}$$

P_A is the elevated pressure within chamber **A**

P_B is the ambient pressure within chamber **B**

V_A and V_B are the gas volumes within chambers **A** and **B** respectively

n_A and n_B are the numbers of moles of gas within chambers **A** and **B** respectively

R is the universal gas constant

T is the temperature of the system

V_S is the skeletal volume of the sample residing in chamber **A**.

When the valve between the chambers is opened, the pressure within the system equilibrates to an intermediate value P_{AB}. V_A and V_B are determined through calibration with spherical tungsten carbide standards and P_A, P_B and P_{AB} are measured by a pressure transducer, thus allowing for accurate calculation of the skeletal volume of the test specimen:

$$V_S = V_A - \frac{V_B}{\frac{P_A - P_B}{P_{AB} - P_B} - 1}$$

Test specimens were run over 10 cycles with 10 purges with a fill pressure of 19.5 psig and an equilibration rate of 0.005 psig min^{-1}. Open porosity is calculated from:

$$p_o = 1 - \frac{V_S}{V}$$

where V is the **bulk volume**, measured using a calibrated *Mitutoyo 293 MDC Lite* micrometer to determine the average length, and radius of a given specimen.

Closed porosity is estimated from:

$$p_c = \frac{\rho}{\rho_S} - \frac{\rho}{\rho_t}$$

ρ_S is the **skeletal density**

ρ is the **bulk density**

ρ_t is the **theoretical density** of a graphite crystal, (2.27 g cm^{-3})

It should be noted that this definition of closed porosity is calculated from a comparison with a perfect graphite crystal and therefore any deviations from the perfect lattice will be considered “closed” porosity. This is generally different from a macroscopic view of what constitutes “closed” porosity (i.e. significant sized porosity with no open route to the sample surface).

Figure 39 shows the pycnometry results for each of the samples tested. The red line shows the variation in skeletal density across the samples measured using pycnometry. Sample bulk densities prior to treatment ranged from 1.05 to 1.34 g cm^{-3}, with skeletal densities ranging from 1.86 to 2.01 g cm^{-3}. The solid black line denotes

the open porosity determined from the bulk and skeletal volumes. The dashed black line shows the closed porosity, calculated from the theoretical crystal density. Only nine of the samples treated in 1% oxygen were selected for measurement after treatment, their skeletal densities are shown by the red points, the open porosity by the black circular points and the closed porosity by the black crosses.

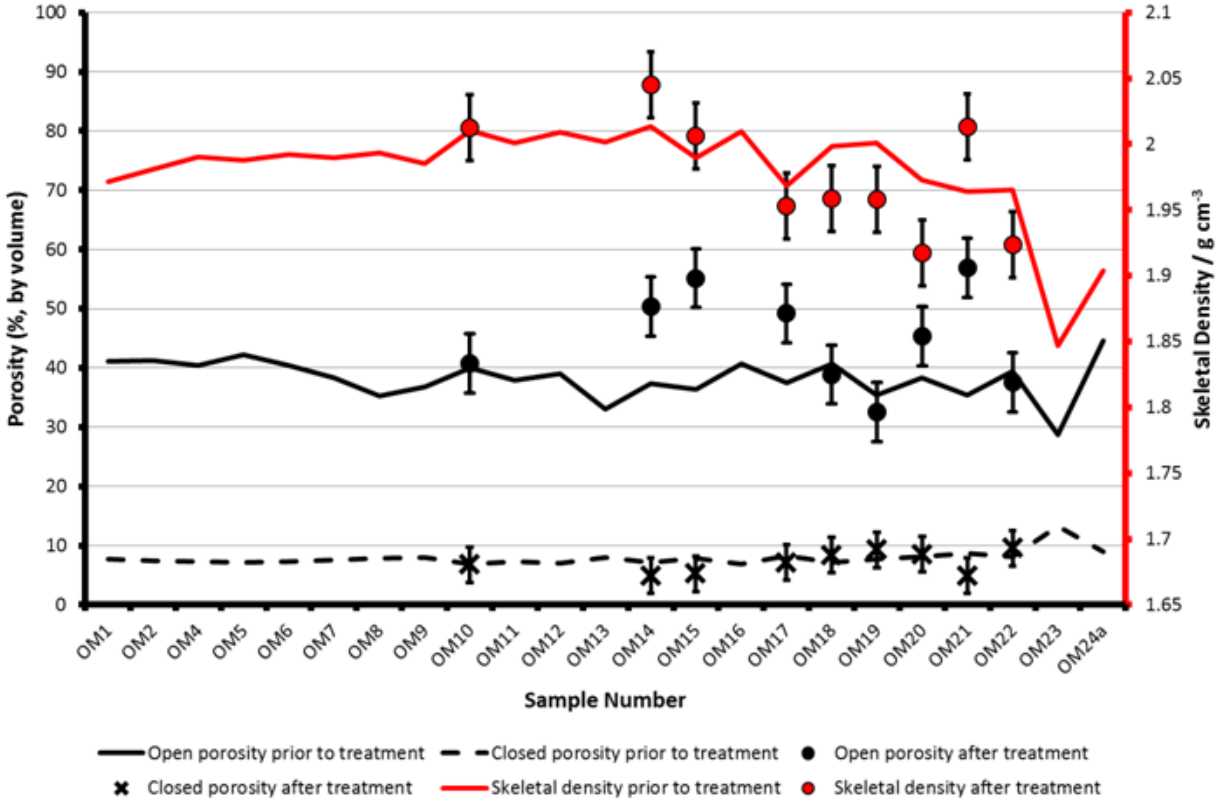

Figure 39 Measured skeletal density and open porosity and estimated closed porosity for each sample prior to treatment. The single points denote the equivalent measures for selected samples after treatment

An increase in open porosity is observed after treatment. This is due to the pitting of the surface of the sample, which generates new open porosity; and to the increase in pore volume of pores exposed to the treatment gas, thus increasing the volume of existing individual pores. The closed porosity remains generally unchanged by the treatment, with such porosity being unaffected by changes at the surface and not experiencing direct contact with the oxidising species during treatment. A small reduction in the volume of closed porosity is detected, which can be explained by the "opening up" of some closed porosity as growing open pores expand and consume them.

The bulk density of the samples falls off rapidly after treatment owing to the increase in open porosity; bulk density reduced in the samples measured from ~ 1.24 g cm^{-3} by on average 0.24 g cm^{-3} after treatment. Skeletal density varies far less in comparison, changing by around 0.04 g cm^{-3} before and after treatment. While bulk density always decreases with such treatment, skeletal density can slightly increase or decrease depending on the type of new porosity which arises. Increases in skeletal density are accompanied by reductions in closed porosity and increases in open porosity as growing open pores envelope smaller closed ones, whereas a drop in skeletal density indicates greater surface oxidation effects.

3.9.1.1 Helium pycnometry glossary

Bulk volume, V	Volume determined by measurement of a body's external dimensions (i.e. $\pi r^2 l$ for a cylinder of radius r and length l). This assumes no internal porosity.
Skeletal volume, V_S	Volume determined by immersion of the body within a fluid. This accommodates any porosity accessible by the liquid.
Bulk density, ρ	Density calculated from: $(mass/V)$.
Skeletal density, ρ_S	Density of sample not including its open porosity (i.e. $mass/V_S$).
Theoretical density, ρ_t	Density of a perfect graphite crystal, determined from X-ray diffraction measurements of lattice parameters as 2.27 g cm^{-3}.
Open porosity, p_o	Internal porosity open to the surface of a body, and thus accessible by fluids during immersion.
Closed porosity, p_c	Internal porosity not open to the surface of a body, and thus inaccessible by fluids during immersion.

3.10 Surface Area

Previous worked carried out within the CARBOWASTE program has attempted to correlate the isotopic release from i-graphite to the porosity and surface area T-4.3.3b. The theory greater the surface area the more likely isotopic release will occur has been tested here with surface area and helium pycnomtery measurements performed pre and post thermal treatment. The direct relationship between porosity and surface area is a fundamental requirement in the interpretation of thermal treatment and isotopic distribution.

The principle behind surface area analysis is that the amount of gas needed to form a monolayer on the surface of a solid material can be determined from the volume of gas absorbed to the surface at different pressures for a constant temperature. The Brunauer, Emmett and Teller (BET) [15-16] equation is used to determine surface area from this technique, however if the absorbed gas is bound persistently in pores with smaller diameters this will affect the rate of desorption and an alternative theory is required to determine the relationship between pore size to pressure change. The BET Equation [16] is given below:

$$\frac{P}{V(P_O - P)} = m\frac{P}{P_O} + b$$

P= Pressure of the absorbed gas

P_O= Saturation vapour pressure

V= Volume of the absorbed gas

m = slope gradient

b= intercept

The Tristar II 3020 (photograph in figure 40) utilises physical adsorption to determine surface area and porosity. Specific surface areas from 0.01 m^2/g can be measured using nitrogen gas and 0.001 m^2/g can be achieved using krypton. The Tristar II 3020 has a gas pressure resolution of 0.005 mmHg and a pressure accuracy of 0.5%. The limitations associated with this technique are that the sample size is small and limited to the vessel geometry therefore must be chosen such that it will fit into the apparatus and must have sufficient surface area in order to give representative results.

Figure 40 Photograph Tristar II 3020

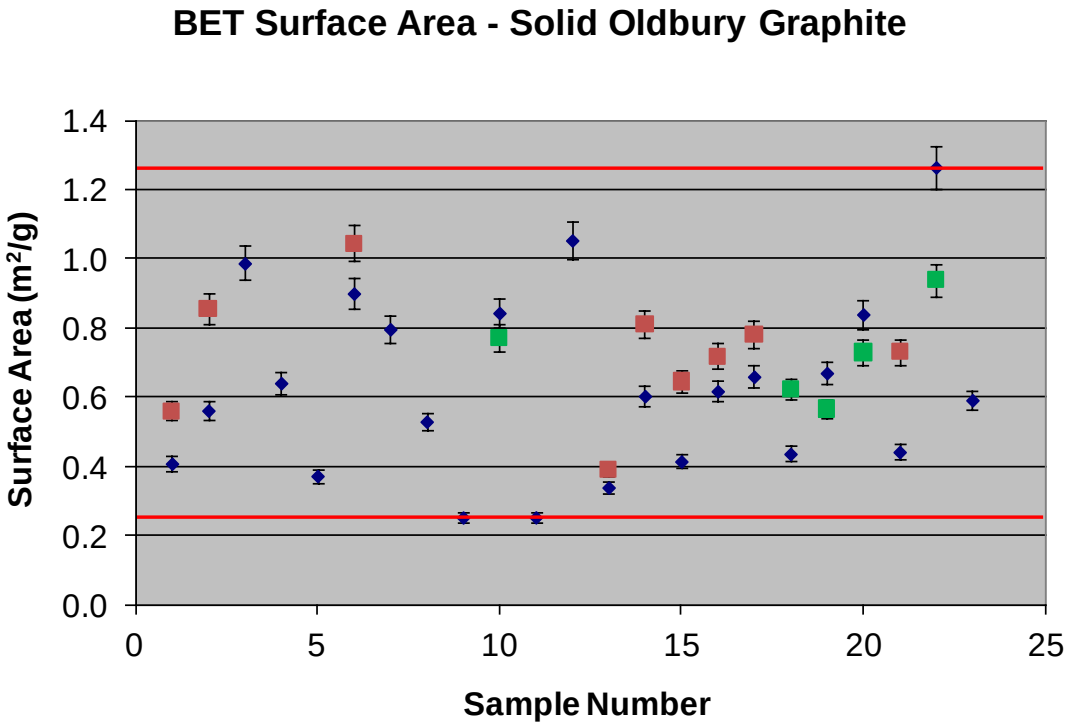

Figure 41 Distribution of surface area analysis performed on all samples

Figure 41 shows the distribution of all the surface area data for the Oldbury i-graphite samples pre and post thermal treatment. The blue diamond's represent pre treated surface area analysis performed on the Tristar, the bold red lines indicate the range of expected spread of nuclear grade graphite surface area as referenced by Nightingale to be in the range from 0.25 – 1.2 m^2/g [17-18]. The green squares represent the surface area analysis of samples treated in Argon gas at 700°C. The red squares represent the surface area of samples treated in 1% O_2 in Agron gas at either 700°C or 800°C. As the solid samples not the powder produced during the 800°C thermal treatment was analysed this indicates that the structure of the material has been eroded but not the full extend observed in figure 23. Previously analysed powdered i-graphite samples from Wylfa reactor had a surface area of 33 m^2/g and virgin PGA powdered graphite had a surface area of 60 m^2/g. Taking this into account had it been possible to analysis the solid and powdered remains of the 800°C thermally treated material the results for these samples may have looked significantly different.

3.11 Conclusions UoM work

The post treatment characterisation techniques which proved interesting accompaniments to this research included gamma spectroscopy and XRD. Possibly for this first time samples were analysed using a gamma spec before and after thermal treatment. The determination of the loss in ^{60}Co during thermal treatment process is a result of significant interest, although steps need to be taken to ensure change in sample geometry is addressed in future research, determining the location of the ^{60}Co will be a great importance for future thermal treatment processes.

The XRD analysis has shown a little impact of the thermal process on the crystallite size, which will hopefully contribute to the understanding of the structure of the i-graphite that remains post thermal treatment with the thermal process seeming almost unambiguous to the carbon structure it has removed.

Issues with sensitivity of using a mixed source (such as i-graphite) have often reduced autoradiography effectiveness/accuracy, as such the experimental data produced is interesting but the swamping effects of gamma isotopes make it little more than a visualisation tool and contamination check.

Limitations also arose with surface area analysis as the 800°C thermally treated samples produced dust/powder which could not be transferred into the glassware without causing a possible contamination risk to the handler. As such an increase in surface area was recorded the author feels the powder produced from the thermal process would have has greatly impacted that data.

Taking observation, surface area and He Pyc analysis into consideration some erosion of the surface structure has occurred during thermal treatment and the difference between 4, 5 and 6 hours runs shows a significant increase in weight loss, sample integrity and percentage isotopic release. Further analysis shows little change in isotopic release between 6 and 8 hour treatment runs under 1% O_2 in argon environment, however the 8 hour treatment run an increase in weight loss was observed for very little additional ^{14}C release.

Tritium release appears to be temperature and oxygen dependant and future experiments will hopefully determine whether a preferential release of tritium can be achieved.

Research at Manchester will continue with experiments into 600°C and 900°C thermal treatment, full isotopic determination of post treated samples and possibly further chemical treatment / leaching of post thermally treated materials.

Unfortunately this data won't be available in time for the CARBOWASTE program however continued efforts at both FZJ and UoM will hopefully result in a journal paper showcasing the completion of this program of work.

4 Summary

Comparison between FZJ and UoM work;

- <30% ^{14}C release under 700°C, 800°C and 1300°C this co-insides with previous chemical treatment experiments performed under T-4.3.3-b.
- What was significantly different between FZJ and UoM data sets was the mass loss of i-graphite. FZJ data indicated mass losses >10% for significant isotopic release for both ^{3}H and ^{14}C. Whereas UoM research indicates mass losses in the region of 22-54% under 1% O_2 conditions and >0.75% under Argon conditions.
- This data supports the previous theory of a non-leachable/non-removal portion of ^{14}C within the structure being in the >70% region however the large difference in weight loss must be attributed to the percentage oxygen the environment and samples.
- ^{3}H temperature dependence shown in FZJ results holds promising value for thermal treatment application in removing mobile isotopic species.

4.1 Publications resulting from this work

- G. Black, L. McDermott, A. N. Jones, B J. Marsden. "Development of an experimental and simulation process to determine the end of life radionuclide inventory of UK irradiated graphite waste". *Modelling and Measuring Reactor Core Graphite Properties and Performance, Birmingham. 31 October – 3 November 2011*
- G. Black, Dr. A. N. Jones, L. McDermott, Prof. B. J. Marsden. "Modelling the Production of Tritium, Carbon-14 and Cobalt-60 in Irradiated Graphite from a UK Magnox Reactor". *MRS, Argentina, 3-7 October 2011*
- R. Holmes, A.N. Jones, L. McDermott, B.J. Marsden 'Development of Surface Marker System for the Observation of microstructural changes in Nuclear Graphite using Micro X-ray tomography'. *MRS, Argentina, 3-7 October 2011*
- A.N. Jones, L. McDermott, B.J. Marsden, T.J. Marrow, and A.J. Wickham. "Characterisation of Irradiated Graphite Waste in Reactor Decommissioning". *Carbon 2009, Biarritz, France, 14 - 19 June, 2009*

5 References

1. Bradbury, D., et al. *Pyrolysis / Steam Reforming and its Potential Use in Graphite Disposal*. in *Proc. 3rd EPRI International Decommissioning and Radioactive Waste Workshop*. 2004. Lyon, France.
2. UKAEA, *GLEEP reactor*.
3. UKAEA, *Reactors UK*. 4th ed. 1969: UKAEA. 116.
4. Podruzhina, T., *Graphite as radioactive waste corrosion behaviour under final repository conditions and thermal treatment.*, in *FZJ Report* 2004: Jülich.
5. von Lensa, W., *CARBOWASTE: New EURATOM Project on 'Treatment and Disposal of Irradiated Graphite and other Carbonaceous Waste'*, in *Proceedings of the 4th International Topical Meeting on High-Temperature Reactor Technology*, HTR2008, Editor. 2008: Washington D.C., USA.
6. Fachinger, J., *14C and 3H Thermal Treatment from Merlin Graphite*, in *CARBOWASTE: 2nd Annual steering committee meeting*, A.N. Jones, Editor. 2009: Marcoule, France.
7. Wickham, A.J. and B.J. Marsden, *Characterisation, Treatment and Conditioning of Radioactive Graphite from Decommissioning of Nuclear Reactors.* IAEA TECDOC-1521,, 2006.
8. Bradtec Decon Technologies, L., *Graphite Decommissioning Options for Graphite Treatment, Recycling, or Disposal, including a discussion of Safety-Related Issues*, E.P.R.I. (EPRI). Editor. 2006.
9. Mason, J.B. and D. Bradbury, *Pyrolysis and its potential use in nuclear graphite disposal*, in *AEA Technical Committee Meeting on "Nuclear Graphite Waste*

Management", I.A.E. Agency, Editor. 1999, IAEA: Manchester, United Kingdom. p. 77-84

10. Fassbender, J., et al., *Die gegenwärtige und zukünftige Nutzung der Forschungsreaktoren FRJ-1 (Merlin) und FRJ-2 (DIDO) der Kernforschungsanlage Jülich. .* Bericht der Zentralabteilung Forschungsreaktoren, 1973.
11. Borchardt, G., *Ergebnisse der Flussdichtemessungen in den Experimentier-Positionen des FRJ-1 und des FRJ-2 nach Leistungserhöhung auf 10 bzw. 25 MW.* Berichte der Kernforschungsanlage Jülich Jül-1022, 1973.
12. Florjan, M., *Dekontamination von Nukleargraphit durch thermische Behandlung*. 2009 reported to year 2012.
13. Canberra, *Genie 2000 Spectroscopy Software: Operations Manual.* 2009.
14. Canberra, *LABSOCS/ISOCS: Operations Manual.* 2009.
15. Seri-Levy, A. and D. Avnir', *The Brunauer-Emmett-Teller Equation and the Effects of Lateral Interactions. A Simulation Study,* Langmuir, 1993. **9**(2623): p. 2523-2529.
16. Brunauer, S., P.H. Emmett, and E. Teller, *Adsorption of Gases in Multimolecular Layers.* 1938. **60**: p. 309-319.
17. Kelly, B.T., *The physics of graphite*. 1981, London: Applied Science Publishers.
18. Nightingale, R.E., *Nuclear Graphite*. 1962, New York: Academic Press.